

Pivot Sébastien (Orcid ID: 0000-0002-8546-7616)

Baroni Mélanie (Orcid ID: 0000-0002-2665-4884)

Bard Edouard (Orcid ID: 0000-0002-7237-8622)

A comparison of ^{36}Cl nuclear bomb inputs deposited in snow from Vostok and Talos Dome, Antarctica, using the $^{36}\text{Cl}/\text{Cl}^-$ ratio

S. Pivot^{1*}, M. Baroni^{1*}, E. Bard¹, X. Giraud¹, ASTER Team^{1,§}

¹*Aix Marseille Univ, CNRS, IRD, INRA, Coll France, CEREGE, Aix-en-Provence, France*

[§]*G. Aumaître, D.L. Boulès, K. Keddadouche*

*Corresponding authors: pivot@cerege.fr; baroni@cerege.fr

KEY POINTS

- Mobility of H^{36}Cl in the Vostok snowpack compared with that of Talos Dome
- $^{36}\text{Cl}/\text{Cl}^-$ ratio isolating stratospheric anthropogenic ^{36}Cl from other sources
- Correspondence between $^{36}\text{Cl}/\text{Cl}^-$ ratio increase and major nuclear bomb tests obtained due to high resolution at Vostok

This article has been accepted for publication and undergone full peer review but has not been through the copyediting, typesetting, pagination and proofreading process which may lead to differences between this version and the Version of Record. Please cite this article as doi: 10.1029/2018JD030200

ABSTRACT

^{36}Cl production in the atmosphere is modulated by the magnetic field intensity of both the Sun and the Earth. The record of ^{36}Cl concentration along with that of ^{10}Be in ice cores may therefore provide information as to their variability. To better understand the ^{36}Cl signal in glaciological archives, we measured its concentration in Talos Dome snow samples (mean accumulation rate of $8 \text{ g.cm}^{-2}.\text{yr}^{-1}$ water equivalent) spanning the 1955 to 1980 C.E. period with a resolution of one sample every 3 years, and in Vostok snow samples (mean accumulation rate of $1.96 \text{ g.cm}^{-2}.\text{yr}^{-1}$ water equivalent) spanning the 1949 to 2007 C.E. period with a six-month resolution that had never before been obtained. Marine nuclear bomb tests in the late 1950s produced anthropogenic ^{36}Cl which was injected into the stratosphere and spread around the globe. In the late 1950s this anthropogenic pulse led to an increase of ^{36}Cl concentration at Talos Dome that was more than 100 times higher than the pre- and post- bomb values. It is noteworthy that the atmosphere of Vostok remains polluted by anthropogenic ^{36}Cl today. This pollution results from gaseous H^{36}Cl mobility at low accumulation sites and implies re-emission of ^{36}Cl from the snowpack that is not observed at Talos Dome. The $^{36}\text{Cl}/\text{Cl}^-$ ratio may be used to discriminate the stratospheric anthropogenic ^{36}Cl source from the tropospheric natural ^{36}Cl source, which allows us to discuss the immobile vs. mobile ^{36}Cl in the Vostok snowpack.

KEYWORDS

- ^{36}Cl
- Antarctica
- HCl mobility
- Nuclear bomb tests
- Cosmogenic nuclides
- Ice core

1. INTRODUCTION

Cosmogenic nuclides such as beryllium 10 (^{10}Be) and chlorine 36 (^{36}Cl) are constantly produced by the interaction of primary and secondary galactic cosmic ray particles with target atoms of the atmosphere. Transferred to the Earth's surface, they accumulate in geophysical reservoirs such as polar ice cores where their concentrations can be measured. The flux of galactic cosmic ray particles reaching the Earth - and therefore the production rates of the cosmogenic nuclides - is modulated by the magnetic field intensities of both the Sun and the Earth, and the variation of their concentration in snow or ice is related to these modulations. ^{10}Be in ice cores has previously been used to reconstruct past solar activity over the last millennium (e.g. (Beer et al., 1988; Raisbeck et al., 1990; Bard et al., 1997; Berggren et al., 2009)). ^{10}Be and ^{36}Cl have both been used to constrain geomagnetic field intensity variations in the past such as, for example, the Laschamp excursion which occurred ~40 ka ago (e.g. (Beer et al., 1992; Raisbeck et al., 1992; Yiou et al., 1997; Baumgartner et al., 1998; Raisbeck et al., 2017)). Compared to ^{10}Be , fewer studies treat ^{36}Cl from glaciological archives, mainly because ^{36}Cl is less abundant than ^{10}Be : the global production $^{10}\text{Be}/^{36}\text{Cl}$ ratio is 11 (Polunin et al., 2016), with the result that a larger sample size is required and measurement by accelerator mass spectrometry is more difficult than for ^{10}Be . In addition, ^{36}Cl is linked to the chlorine geochemical cycle and can be found in both a particulate (Na^{36}Cl) and a gaseous (H^{36}Cl) phase, which involves different atmosphere/snow transfer. The ^{10}Be geochemical cycle is simpler than that of ^{36}Cl because ^{10}Be atoms need to attach to aerosols in order to fall to the Earth's surface. The increase in aerosols load after stratospheric volcanic eruptions can cause an increase in the ^{10}Be deposition flux (Baroni et al., 2011, 2019). ^{10}Be is also influenced by atmospheric circulation (Baroni et al., 2011; Pedro et al., 2012; Miyake et al., 2019). The comparison of ^{10}Be and ^{36}Cl makes it possible to leave

out their specific geochemical cycles in order to better isolate the signal related to their production in the atmosphere. The aim of this study is to better understand the ^{36}Cl cycle and ^{36}Cl deposition in Antarctica.

2. CURRENT STATE OF CHLORINE KNOWLEDGE IN ANTARCTICA

2.1 ^{36}Cl production and distribution in the atmosphere

In natural conditions, ^{36}Cl ($T_{1/2} = 301 \pm 2$ ka (Bentley et al., 1986)) is produced in the atmosphere through the spallation of ^{40}Ar atoms. Its mean global production rate is 2.5×10^{-3} $\text{at.cm}^{-2}.\text{s}^{-1}$ (Poluianov et al., 2016), with an enhanced production rate in the polar atmosphere (stratosphere and troposphere) that reaches 5.6×10^{-3} $\text{at.cm}^{-2}.\text{s}^{-1}$. As with ^{10}Be , the main ^{36}Cl reservoir is located in the stratosphere rather than in the troposphere, due to both the higher production rate (e.g. (Masarik & Beer, 1999; Poluianov et al., 2016)) and the longer residence time of ^{10}Be and ^{36}Cl which is estimated at 1 to 2 years in the stratosphere (Raisbeck et al., 1981; Heikkila et al., 2009a). This allows ^{10}Be and ^{36}Cl to accumulate, unlike in the troposphere where the residence time is to the order of a few weeks before ^{36}Cl and ^{10}Be are washed out through dry and wet depositions (Bentley et al., 1982).

Besides its natural source, ^{36}Cl also has an anthropogenic source related to the marine nuclear bomb tests from the 1950s to the early 1970s which produced large amounts of anthropogenic ^{36}Cl . Anthropogenic ^{36}Cl is produced through the capture of thermal neutrons emitted during the nuclear bomb tests by ^{35}Cl from sea salt (NaCl) (Bentley et al., 1982; Elmore et al., 1982; Heikkila et al., 2009b). Anthropogenic ^{36}Cl production is tightly linked to marine nuclear tests as seawater is the only source of chloride able to produce sufficient ^{36}Cl to be globally recorded (Bentley et al., 1982). This is not the

case for some other nuclides (as for example cesium 137 (^{137}Cs) and tritium (^3H)), which were produced mainly during atmospheric and terrestrial nuclear tests. The marine tests, primarily performed on atolls or barges, were initiated by the USA in the Pacific Ocean on Enewetak and Bikini Atolls (11.3°N) between 1952 and 1958 (Table 1). These were followed by tests on Christmas and Johnston Islands (2°N and 17°N, respectively) in 1962. Marine testing ended with the French events on Mururoa and Fangataufa Atolls (21.5 and 22.1°S, respectively) between 1968 and 1974 (Table 1). The intensity of these marine nuclear tests permitted ^{36}Cl to reach the stratosphere, where it is thought to be in gaseous form (Zerle et al., 1997), then to be distributed across the globe before finally transferring to the troposphere. Consequently, the resulting ^{36}Cl pulse can be observed in both low and high latitude ice cores from African (Thompson et al., 2002), Asian, Alpine, Andean (Heikkila et al., 2009b), and North American (Green et al., 2000) glaciers, as well as in ice cores from Greenland and Antarctica (Elmore et al., 1982; Synal et al., 1990; Delmas et al., 2004; Heikkila et al., 2009b). These observations have permitted to estimate the mean stratospheric residence time of anthropogenic ^{36}Cl at approximately 3 to 4 years (Heikkila et al., 2009b). This residence time is higher than the 2 years required by naturally produced ^{36}Cl because first, most of the marine nuclear bomb tests occurred near the equator, which increases the time transfer to higher latitudes where natural ^{36}Cl is mainly produced (Heikkila et al., 2009b), and second, because the exchanges between the stratosphere and the troposphere are maximum at high latitudes (Heikkila et al., 2009a). Approximately 80 kg of ^{36}Cl was injected into the stratosphere between 1952 and 1971, resulting in a higher ^{36}Cl deposition flux (100 to 1000 times higher than the natural ^{36}Cl deposition flux) in low latitude glaciers or Greenland and Antarctica (Heikkila et al., 2009b).

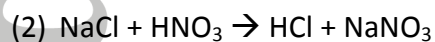
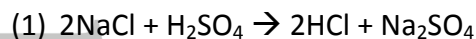
2.2 Chlorine transport and mobility in snow

Post-depositional chlorine mobility

Following the end of marine nuclear bomb testing, ^{36}Cl returned to near pre-bomb levels in glaciological archives in the 1980s (Elmore et al., 1982; Heikkila et al., 2009b), except at Vostok in Antarctica (Delmas et al., 2004). This has been explained by the mobility of ^{36}Cl in its gaseous form (H^{36}Cl), in firns at low accumulation sites located on the High Antarctic Plateau, such as Vostok (Delmas et al., 2004). ^{36}Cl mobility is not observed at the Dye 3 and NGRIP sites in Greenland (Delmas et al., 2004; Heikkila et al., 2009b), and is limited at Berkner Island in Antarctica (Heikkila et al., 2009b). This may be explained by the higher accumulation rates for these sites compared to Vostok. Snow pit studies at Dome C (Legrand & Delmas, 1988; Röthlisberger et al., 2003; Benassai et al., 2005) and at Vostok (De Angelis & Legrand, 1995; Wagnon et al., 1999) evidence an increase of Cl^- concentration from the bottom to the surface along the first meters, which can be attributed to post-depositional mobility. Such a pattern is only evidenced at sites with accumulation rates lower than 4 to 8 $\text{g}\cdot\text{cm}^{-2}\cdot\text{yr}^{-1}$ water equivalent (De Angelis & Legrand, 1995; Röthlisberger et al., 2003; Benassai et al., 2005). Higher accumulation rates may preserve HCl in snow and may therefore preserve both the deposited anthropogenic and the natural H^{36}Cl (Delmas et al., 2004; Benassai et al., 2005; Heikkila et al., 2009b). Post-depositional mobility only affects HCl because of its lower vapor pressure as it is a gas, contrary to NaCl which is an aerosol, i.e. a solid. The outcome of the Delmas et al. (2004) study underlines the difficulty of using ^{36}Cl at low accumulation rate sites due to the mobile fraction which may limit the interpretation for past solar activity and geomagnetic activity reconstruction.

Chlorine transport and fractionation in Antarctica

In Antarctica, chlorine originates primarily from the emission of NaCl during sea ice formation (Wagenbach et al., 1998; Rankin et al., 2004) and from the open sea (Hall & Wolff, 1998; Hara et al., 2004), before being carried by wind across Antarctica. The percentage of NaCl vs HCl deposited in snow depends on the site characteristics and, in particular, on both the distance from the ocean and the altitude of the site, since marine aerosols will age with distance from the source and be fractionated while reacting with acidic species in the atmosphere. Fractionation is a chemical reaction of nitric and sulfuric acids (HNO₃ and H₂SO₄) with sea salt NaCl to form HCl (Legrand & Delmas, 1988), according to the following reactions:



The newly formed sodium nitrate (NaNO₃) and sodium sulfate (Na₂SO₄) remain in aerosol form. The degree of fractionation (in %) from NaCl to HCl is expressed by the Cl⁻/Na⁺ ratio and represents the portion of the initial NaCl that is transformed during transport according to reactions (1) and (2), with the residual portion remaining in the NaCl form. The natural Cl⁻/Na⁺ sea water weight ratio is estimated at 1.9 at the emission source, with fluctuation from 1.8 in summer to 2 in winter (Legrand et al., 2017). The higher winter values are due to mirabilite (Na₂SO₄) precipitation from frost flowers when sea ice is formed (Rankin et al., 2000), as Na⁺ is lost from the brine. A ratio of 1.9 indicates no fractionation and the percentages increase as the ratio moves towards zero.

At the coastal site of Dumont D'Urville (Antarctica), the degree of fractionation is 10% year round (Jourdain & Legrand, 2002) meaning that NaCl is well preserved, while at the

inland site of Dome C, it is 60 % ($\text{Cl}^-/\text{Na}^+ = 0.7$) on a yearly average, with variations from 40 % ($\text{Cl}^-/\text{Na}^+ = 1.2$) in winter to 95 % ($\text{Cl}^-/\text{Na}^+ = 0.1$) in summer (Legrand et al., 2017). The difference in fractionation between Dome C and Dumont D'Urville is due to the distance from the sources, with older marine air masses at inland sites compared with coastal sites ((Hara et al., 2014), see Figure 1 for location of the sites). The seasonal variation observed at Dome C is due to acidic species (mostly sulfate, available in large particles in the atmosphere during summer), enhancing reaction (1) (Legrand et al., 2017).

At Dome Fuji (inland Antarctica, altitude 3810 m), less than 10% of the initial NaCl remains (Iizuka et al., 2012, 2016) because of a larger amount of SO_4^{2-} introduced through the stratospheric-tropospheric exchanges as opposed to at lower altitudes (Iizuka et al., 2016). However, the amount of dust may limit the degree of fractionation at these altitudes, as dust neutralizes acidic species (Oyabu et al., 2016). In the modern period, the level of dust is low and sea salt is modified during transport, which implies that the chloride arriving on the central Antarctic plateau is mainly in the HCl form (Legrand et al., 2017).

Until now, ^{36}Cl measurements have been reported at only four sites in Antarctica, i.e. Vostok, Berkner Island, Dome Fuji and Allan Hills (Finkel et al., 1980; Nishiizumi et al., 1983; Delmas et al., 2004; Heikkila et al., 2009b; Sasa et al., 2010). It is for this reason that the study of anthropogenic ^{36}Cl may provide unprecedented information on the Cl^- geochemical cycle in Antarctica and a better understanding of Cl^- preservation in the ice at low accumulation sites.

To test this, we studied a snow pit dug at Vostok 10 years after the pit sampled by Delmas et al. (2004). Our objective was to follow the evolution of anthropogenic ^{36}Cl in

snow so as to ascertain if all anthropogenic ^{36}Cl is subject to mobility or if, on the contrary, a portion of it is preserved in the snowpack. In parallel, ^{36}Cl analyses were conducted on an ice core from Talos Dome, where accumulation is thought to be high enough to preserve chlorine as NaCl and HCl, and which also spans the period of nuclear bomb tests. The comparison between these contrasted sites provides a better understanding of the transport of anthropogenic ^{36}Cl , of its chemical form (Na^{36}Cl vs. H^{36}Cl), and also supplies information on how chlorine is recorded in the snowpack.

3. MATERIAL AND METHODS

The studied snow pit is located near the Vostok station, on the East Antarctic Plateau (78°S, 106°E, 3488 m, -55°C on average; see Figure 1 for location). ^{10}Be , major ions, radio activity (beta and gamma), ^3H and water oxygen isotopes have previously been measured (Baroni et al., 2011; Winkler et al., 2013; Fourné et al., 2018) in this snow pit. The mean accumulation rate is $1.96 \text{ g}\cdot\text{cm}^{-2}\cdot\text{yr}^{-1}$ water equivalent (Ekaykin et al., 2004). The pit was dug in 2008 down to a depth of 3.65 m, and covers approximately the 1949 to 2008 C.E. period (for details of the chronology refer to Baroni et al. (2011)). It thus spans the marine nuclear testing period. For this study, the ages are all expressed in Common Era (C.E.).

A total of 104 samples were prepared for ^{36}Cl measurements. After removing 100 g from the initially melted snow sample for ^{10}Be analysis, the remaining water was frozen in clean bottles for ^{36}Cl analysis. Some samples from the upper and deeper parts of the snow pit, i.e. the parts outside the period of nuclear bomb testing, were grouped together because of their expected low ^{36}Cl concentration. These samples were initially collected at ~ 3 cm intervals along the snow pit to perform the ^{10}Be analysis. The other samples were analyzed

for their ^{36}Cl concentration with the same resolution as for ^{10}Be . The concentration of major ions (chloride and sodium for this study) had previously been measured by Baroni et al. (2011), but since the samples were stored frozen for 6 years in airtight bottles, 16 of 104 samples were analyzed in the frame of this study using ion chromatography at the IGE (Institut des Géosciences de l'Environnement, Grenoble, France) (Ginot et al., 2014) to identify possible variations of the concentration during storage.

In addition, 13 samples from the Talos Dome ice core (72°S, 159°E, 2316 m, -41°C on average; Figure 1 for location) were processed for measurement of ^{36}Cl concentration. The mean accumulation rate of this core is $8 \text{ g}\cdot\text{cm}^{-2}\cdot\text{yr}^{-1}$ water equivalent (Stenni et al., 2011; Caiazzo et al., 2016). The core was drilled in 2007 in the framework of the European "TALDICE" project: it is 1620 m long and spans more than 150 ka (Bazin et al., 2013; Veres et al., 2013). The first 5 meters of the core were not available for analysis, so testing covered only the samples located between 5.25 m and 16.5 m, spanning the 1910 to 1979 period (chronology based on the WD2014 timescale (Sigl et al., 2016)). One measurement was performed for every 3 years between 1947 and 1979 (~150 g of regrouped snow samples), and one every 12 years between 1910 and 1935 (~680 g of regrouped snow samples). During the chemical preparation for ^{10}Be measurements, the samples were passed through a cation exchange column which retained Be^{2+} in the resin but not Cl^- . The solution was stored in clean bottles kept frozen prior to measurement of ^{36}Cl concentration. Of the 13 samples, 9 were also analyzed by ion chromatography at IGE to measure the concentration of major ions (Ginot et al., 2014).

After being precipitated as AgCl (see the detailed protocol in Supplementary Materials, 7.1), the samples were measured using the 5MV French AMS national facility ASTER, installed at CEREGE (Arnold et al., 2013). ^{36}Cl concentration was determined from the measured

$^{36}\text{Cl}/^{35}\text{Cl}$ ratio, while the $^{35}\text{Cl}/^{37}\text{Cl}$ ratio enabled to determine Cl^- concentration by isotopic dilution (Bouchez et al., 2015). ^{36}Cl concentration was corrected from Cl^- natural concentration values determined by isotopic dilution. The accuracy of ^{36}Cl and Cl^- measurements at ASTER has previously been validated through comparison of measurements performed on Dome C snow samples at ASTER and DREAMS, a 6MV AMS facility located in Dresden, Germany (Braucher et al., 2018). In this study, the comparison of Cl^- concentrations determined by isotopic dilution and ion chromatography on the same samples showed that the concentrations measured and calculated using these two independent methods were consistent (see Supplementary Materials 7.3).

4. RESULTS AND DISCUSSION

4.1 Cl^- and Cl^-/Na^+ from Vostok and Talos Dome records

The Cl^- concentration at Talos Dome ranges from 81 to 203 ppb, with values increasing from 1960 to 1980 (Figure 2E, blue line). The Na^+ concentration also increases during this time interval, with values ranging from 50 to 150 ppb (Figure 2E, gold line). However, the Cl^-/Na^+ ratio does not vary from 5 to 16.5 m and remains constant at Talos Dome, with an average value of 1.84 ($\sigma = 0.13$) (Figure 2F). The stable Cl^-/Na^+ ratio measured at Talos Dome is in agreement with the yearly averaged natural ratio from the ocean, estimated at 1.90 ± 0.20 by Legrand et al. (2017), meaning either that fractionation is negligible at Talos Dome, or that all the deposited chlorine (NaCl and HCl) is preserved in the snowpack.

At Vostok, the Cl^- concentration shows a gradual increase from the deepest part of the snow pit to the top (Figure 2B, blue line). The values are roughly constant at 20 ppb

from 1949 to 1962 (from 3.6 to 2.9 m depth), then increase with internal variability until they reach 180 ppb at the top of the snow pit (Figure 2B). However, such an increase is not evidenced regarding sodium concentration, which exhibits constant values close to 24 ppb ($\sigma = 11$ ppb) throughout the entire snow pit (Figure 2B, gold line). This implies values of the Cl^-/Na^+ ratio higher than 10 at the top of the snow pit (Figure 2C), which is well above the marine seawater ratio of 1.9 (Legrand et al., 2017), while below 2.9 m the ratio is 0.76 on average (Figure 2C). The high values of the Cl^-/Na^+ ratio close to the surface indicate that there is more chloride than expected in the first meters. According to Wagon et al. (1999), this results from an increase in the Cl^- concentration toward the surface which can be explained by HCl mobility in snow. Gas migration in polar ice has also been evidenced for other elements, such as nitric acid (HNO_3 , (Mayewski & Legrand, 1990)), or methanesulfonic acid (MSA, Osman et al., 2017)). Both the HCl migrating from the deeper part of the snow pit and the newly deposited chlorine will thus accumulate within the upper meters (Figure 2B, blue line). This is consistent with observations made concerning the atmosphere at Dome C, where the gaseous HCl concentration was found to be 3.4 times higher than the concentration of chloride in the aerosol phase (Legrand et al., 2017). This excess of the gaseous phase may be due to more efficient transport of gaseous chloride from the ocean to Dome C compared to sea salt, and/or to the re-emission of a large quantity of HCl from the snowpack which would be a source over the Antarctic Plateau (Legrand et al., 2017). For comparison, if a gaseous/aerosol ratio of 3.4 (as found in the atmosphere at Dome C (Legrand et al., 2017)), and a Cl^- concentration as NaCl set at 10 ppb from Wagon et al. (1999) were applied, the HCl concentration at Vostok would be 34 ppb (using the 3.4 value ratio), and the total chloride concentration would be approximately 45 ppb. This estimate is 4 times lower than the concentration of 180 ppb measured at the top of the Vostok snow

pit. This may result either from the accumulation of HCl in the first meters of Vostok before being re-emitted, and/or from a higher HCl concentration in the atmosphere at Vostok than at Dome C.

No HCl post-depositional mobility is observed at sites with higher accumulation rates, such as South Pole and Talos Dome (Whitlow et al., 1992; Benassai et al., 2005), because high accumulation rates may prevent HCl from escaping from the snowpack.

The mobility of chlorine as HCl in the first few meters of the snowpack at Vostok may also influence part of the anthropogenic ^{36}Cl as H^{36}Cl , as opposed to a non-mobile Na^{36}Cl phase.

Contrary to what is observed at the surface at Vostok, the Cl^-/Na^+ ratio below 2.9 m depth is 0.76 on average, which corresponds to a sea-salt fractionation of approximately 60%. The Cl^- concentration of 20 ppb in the deepest part of our snow pit at 3.65 m depth is twice as high as that measured by Wagnon et al. (1999) below 6 m depth at Vostok, leading to a Cl^-/Na^+ ratio of 0.4. A value of 0.4 corresponds to a fractionation of approximately 80%, higher than the 60% found in our study. The 20% difference between the two studies suggests that gaseous chloride persists at 3.65 m depth but has been lost at 6 m depth, and that only the NaCl component remains below. This hypothesis is supported by observations made at Dome C, where the Cl^-/Na^+ ratio of 0.58 measured in the firn between 10 and 50 m depth is similar to the value of 0.7 observed in aerosols collected at Dome C during the 2006 - 2016 period (Röthlisberger et al., 2003; Legrand et al., 2017).

4.2 ^{36}Cl nuclear imprint

4.2.1 ^{36}Cl signal at Talos Dome

The ^{36}Cl concentration measured at the Vostok and Talos Dome sites is presented in Figures 2A and 2D, respectively, and the ^{36}Cl fluxes are shown in Figure 3. At Talos Dome, the ^{36}Cl concentration is $2.30 \times 10^3 \text{ at.g}^{-1}$ between 1910 and 1950, then increases by a factor of 100 to a maximum of $2.59 \times 10^5 \text{ at.g}^{-1}$ in around 1955, before decreasing steadily since then to reach a concentration of $9.30 \times 10^3 \text{ at.g}^{-1}$ in 1979 (Figure 2D), which is 4 times higher than before 1950. The ^{36}Cl flux profile is similar to that of ^{36}Cl concentration. An increase of a factor of 100 in ^{36}Cl concentration and ^{36}Cl flux cannot be attributed to natural ^{36}Cl production but rather to anthropogenic ^{36}Cl produced from marine nuclear bomb tests. The same amplitude is observed at Berkner Island (Figure 3, (Heikkila et al., 2009b)), a site located in the Weddell Sea in Antarctica (see Figure 1).

A similar evolution is observed in ^{36}Cl fluxes when comparing Talos Dome and Dye 3 in Greenland (Synal et al., 1990), where an increase from 1948 to 1956 followed by a slow decrease since then (Figure 3) has been observed. The increase in ^{36}Cl flux is 10 times higher at Dye 3 than at Talos Dome over the 1947 to 1979 period. This may be explained by the fact that most of the nuclear tests occurred in the Northern Hemisphere (Table 1), inducing a higher anthropogenic ^{36}Cl flux than in Antarctica. This difference in deposition between Greenland and Antarctica is consistent with previous ^{137}Cs , ^{90}Sr and ^{240}Pu concentration measurements in Greenland and in Antarctica. Indeed, the fluxes of ^{137}Cs , ^{90}Sr and ^{240}Pu are 7.6, 6 and 7.5 times higher, respectively, at Dye 3 (Greenland) than at J-9, a site located in the Ross Sea in Antarctica (Koide et al., 1979). ^{137}Cs , ^{90}Sr and ^{240}Pu deposition in fresh snow is related to the atmospheric thermonuclear tests that occurred between 1955 and 1980.

Two main ^{137}Cs , ^{90}Sr and ^{240}Pu peaks at 1955 and 1965 have been well identified in Antarctic snow (Feely et al., 1966; Koide et al., 1977, 1979; Pourchet et al., 1997, 2003). These peaks are used as time markers because ^{137}Cs , ^{90}Sr and ^{240}Pu are immobile tracers associated to the particulate phase in snow.

The peaks in ^{36}Cl flux around 1955 at Talos Dome and Dye 3 are also in phase, while a time lag is observed at Berkner Island where the maximum ^{36}Cl flux is reached later (Figure 3). This time lag between Dye 3 and Berkner Island can be explained by sublimation which produces gaseous ^{36}Cl (Heikkila et al., 2009b), despite an accumulation at Berkner Island which exceeds the accumulation rate of $8 \text{ g}\cdot\text{cm}^{-2}\cdot\text{yr}^{-1}$ determined as the limit at which HCl preservation in snow can be assumed by Benassai et al. (2005). However, the Cl^-/Na^+ ratio of 1.94 (Mulvaney et al., 2002) agrees with the sea water Cl^-/Na^+ reference ratio of 1.90 ± 0.2 (Legrand et al., 2017), suggesting good preservation of chlorine. Possible explanations for this ~ 4 year time lag between Talos Dome/Dye 3 and Berkner Island include chronological uncertainty and the different resolutions of the two snow pits.

The stable Cl^-/Na^+ ratio at Talos Dome and the comparison with the profiles of ^{36}Cl flux at Dye 3 and Berkner Island during the period of nuclear bomb tests show that chlorine and ^{36}Cl are well preserved at Talos Dome.

4.2.2 ^{36}Cl signal at Vostok

The Vostok record also exhibits an increase in ^{36}Cl concentration by a factor of 15 from $1.70 \times 10^4 \text{ at}\cdot\text{g}^{-1}$ in 1949.5 to two maxima of $2.41 \times 10^5 \text{ at}\cdot\text{g}^{-1}$ and $2.76 \times 10^5 \text{ at}\cdot\text{g}^{-1}$ at around 1968 and 1979, respectively. A ^{36}Cl concentration increase to $2.14 \times 10^5 \text{ at}\cdot\text{g}^{-1}$ is also observed in 1957 at Vostok (see discussion section 4.3.1) (Figure 2A). The increase in ^{36}Cl

concentration is less pronounced and is delayed at Vostok compared with Talos Dome. The decrease in ^{36}Cl concentration after the maxima is also slower (Figure 2A). It can be hypothesized that natural ^{36}Cl levels are not observed at Vostok compared to the Talos Dome record, which goes back to 1910. The Vostok ^{36}Cl concentration expected from natural ^{36}Cl production can be estimated at $6.71 \times 10^3 \text{ at.g}^{-1}$ using the mean ^{10}Be concentration of $7.65 \times 10^4 \text{ at.g}^{-1}$ measured in the same snow pit (Baroni et al., 2011) and the theoretical $^{10}\text{Be}/^{36}\text{Cl}$ production ratio of 11.4 (Poluianov et al., 2016). ^{36}Cl concentration in the deepest part of the snow pit (i.e. $1.70 \times 10^4 \text{ at. g}^{-1}$ in 1949) is still more than twice as high as the estimated natural ^{36}Cl concentration, and more than 10 times higher at the top of the snow pit (e.g. $7.48 \times 10^4 \text{ at. g}^{-1}$ in 2007).

As already shown by Delmas et al. (2004) regarding a snow pit dug at Vostok in 1998, the mobility of anthropogenic H^{36}Cl affecting the first meters of the Vostok record is clearly evidenced when comparing ^{36}Cl with ^{137}Cs radionuclide measurements performed in the same snow pit (Baroni et al., 2011) (Figure 4A green line and Figure 4B). Even if ^{137}Cs and ^{36}Cl were produced during different nuclear bomb tests, atmospheric for the former and marine for the latter, they can be compared because they were performed during the same period. The two ^{137}Cs peaks are well identified in 1955 and 1965, after which ^{137}Cs concentration decreases rapidly, returning to natural levels by 1972 (Figure 4B). Such a pattern is not observed in ^{36}Cl concentration evolution at Vostok, where no return to the pre-bomb concentration after the end of the nuclear tests is observed, not even at the top of the core corresponding to 2007 (Figure 4A). These differences are also visible with tritium, which is related to the water vapor cycle in the stratosphere. Tritium is another marker of nuclear testing whose concentration tends towards pre-bomb concentrations soon after the end of the tests ((Fouéré et al., 2018), Figure 4C). Migration of H^{36}Cl within

the first meters of the Vostok snow pit has also been confirmed by the $^{10}\text{Be}/^{36}\text{Cl}$ ratio. Its value of 1.13 at the top of the snow pit is significantly lower than the expected polar production value of 11.4 (Poluianov et al., 2016). This means that the 1949-2008 period is entirely affected and polluted by anthropogenic ^{36}Cl , probably when it is in the form of gaseous HCl as discussed in Section 4.1, thus prohibiting a return to the natural level during this time period at Vostok. Along the record affected by mobility, ^{36}Cl concentration also shows some variability, with observable isolated increases after 1980 (Figure 2A) in particular. This may be related to an immobile ^{36}Cl signature (see discussion 4.3.2).

After having demonstrated that only Vostok is affected by the mobility of a fraction of H^{36}Cl , a phenomenon not observed in other Antarctic and Greenlandic sites with higher accumulation rates, we compared our Vostok record to that of Delmas et al. (2004) to evidence the evolution of the ^{36}Cl concentration as a function of depth during the ten years separating the two studies.

4.2.3 ^{36}Cl evolution in ten years at Vostok

Before any comparison, the depth scales of the snow pits sampled in 1997 and 1998 (Delmas et al., 2004) and in 2008 (this study) were adjusted using the ^{137}Cs concentrations measured along them in order to take into account the snow accumulated between these two sampling periods (e.g. between 1998 and 2008). Furthermore, while comparing the 1997 and 1998 snow pits (Delmas et al., 2004), we observed that the second ^{137}Cs peak was not related to the 1955 event, but rather to the intermediate one, also recorded by Baroni et al. (2011). We therefore shifted the depth scales of the 1997 and 1998 snow pits down by

49 cm to adjust their chronologies to the 2008 snow pit. For this comparison, we chose to use only the 1998 snow pit which covers a longer time period than does the 1997 snow pit. ^{36}Cl concentration profiles as a function of time from the 1998 and 2008 snow pits exhibit differences, highlighting that a part of the ^{36}Cl initially deposited suffered from post-depositional disturbances. Indeed, during the ten year lapse between the two records, the two main ^{36}Cl peaks migrated toward the surface, i.e. toward more recent years (Figure 4A, green and black lines). Below 2.9 m depth corresponding to the 1949 - 1962 period, the ^{36}Cl budget is similar between the two studies, implying no significant loss or gain of ^{36}Cl (Figure 4A). These observations suggest that part of the deposited ^{36}Cl signal is preserved below 2.9 m. Over the 1976 - 1998 period, the integrated ^{36}Cl inventory is twice as high in our study than in the Delmas et al. (2004) record, while over the 1962 - 1976 period it is 20% lower (Figure 4). This observation raises the question of the consequences of the one-directional mobility of H^{36}Cl toward the surface and its subsequent re-emission to the atmosphere. The total balance over the 1962 - 1998 period is, however, 27% higher in our study than in Delmas et al. (2004). This may be explained by uncertainties associated with the dating of the snow pit in Delmas et al. (2004), whose chronology is based on the ^{137}Cs peaks only, while we use these time markers in addition to markers of two volcanic eruptions (the 1963 Agung event and the 1991 Pinatubo eruption), as based on the sulfate record. The resolution is also lower in Delmas et al. (2004) compared to our work. As illustrated by Delmas et al. (2004) in their study of 1997 and 1998 Vostok snow pits, this may also be explained by concentration profile differences along different snow pits from the same site, even if the pits are dug close to each other. This may also highlight the fact that anthropogenic ^{36}Cl is still being deposited in Vostok. It has recently been observed that HCl concentration is twice as high as the amount of chloride lost by sea-salt aerosol in the

atmosphere at Dome C, suggesting that HCl released by the snowpack may be a significant source of chlorine over the Antarctic Plateau (Legrand et al., 2017). If HCl can be re-emitted to the atmosphere from low accumulation sites of the East Antarctic Plateau, anthropogenic H^{36}Cl can also be re-emitted and may be transported via atmospheric circulation to Vostok, thus creating a positive mass balance compared with the snow pit of 1997 studied by Delmas et al. (2004).

4.2.4 Model simulation of ^{36}Cl evolution in 10 years

Considering the ^{36}Cl concentration profile of Delmas et al. (2004) as initial conditions (Figure 4A, black line), an advection-diffusion scheme can then be applied to this profile to simulate its evolution from 1998 to 2007. We have assumed that new layers of snow were free of ^{36}Cl when deposited during this time interval. Three model results are presented.

First, we applied the advection-diffusion coefficients as presented in Delmas et al. (2004), i.e. an upward advection of $5 \text{ cm}\cdot\text{yr}^{-1}$ and a diffusion coefficient of $0.0025 \text{ m}^2\cdot\text{yr}^{-1}$ (Figure 4A, orange line). In this case, the ^{36}Cl concentrations of the model (orange line) fail to reproduce the data (green line). The sharp increase observed around 1962 rises toward the surface by about 6 years in the model, whereas there is almost no observed shift between the two experimental snow records of 1998 and 2007. The double-peak structure vanishes, mostly under the influence of the strong diffusion. This suggests that the advection and diffusion coefficients used by Delmas et al. (2004) require adjustment.

For this purpose, we optimized the advection-diffusion parameters through the comparison of the modeled profile to the experimental profile of 2008. The multiple iterations allowing to minimize the root mean square of differences (RMSD) led to a new set of parameters: an upward advection of $3.9 \text{ cm}\cdot\text{yr}^{-1}$ and a diffusion coefficient of $0.0132 \text{ m}^2\cdot\text{yr}^{-1}$ (Figure 4A, red

line). Using this new set of parameters, the modeled ^{36}Cl concentration is lower than the experimental ^{36}Cl concentration (green line) over the entire sequence, except between 1973 and 1977 (Figure 4A). Here again, the diffusion is strong and smooths the double-peak structure. The ^{36}Cl concentration at the surface is still underestimated. It can also be observed that for the layers between 1930 and 1959, ^{36}Cl concentration remains unchanged (comparison of black and red curves). In this part of the record, diffusion pushes the signal toward greater depths (gradient from higher to lower concentrations) whereas advection is directed toward the surface: the two processes of advection and diffusion counteract each other, leading to an apparent stability of the record. More importantly, this particular simulation emphasizes the fact that the amount of ^{36}Cl cumulated in the snow profile in 1998 is not sufficient in comparison to the amount present in 2007. In our hypothesis above, we postulate that anthropogenic ^{36}Cl may be partially re-emitted into the atmosphere (a process not included in the model) at Vostok itself or at nearby Antarctic sites before being transported to Vostok, and it may also be redeposited in the first meters of the firn, explaining the higher ^{36}Cl concentration in the more recent years of the 2007 record compared to the model. The Vostok atmosphere may thus remain polluted by anthropogenic H^{36}Cl today. This phenomenon of re-emission and deposition is the same as for HCl along the first meters of the firn (see discussion above) which would explain why natural ^{36}Cl levels have not yet been reached today and why ^{36}Cl concentrations in the top layers of the firn increased from 1998 to 2007.

A third modeling experiment was conducted by considering a moderate advection velocity of $3.9 \text{ cm}\cdot\text{yr}^{-1}$ as in the previous experiment, and a diffusion coefficient reduced by a factor of 10, i.e. $0.00025 \text{ m}^2\cdot\text{yr}^{-1}$ (Figure 4A, purple line). This combination of parameters allows to maintain the double-peak structure, which shifts toward the surface by a reasonable depth

compared to the data. However, the sharp increase around 1962 also shifts toward the surface (whereas it should not) and concentrations in the top layers remain underestimated. No simple combination of advection-diffusion parameters was able to satisfy the transformation of the experimental record from 1998 to 2007.

The central aspect of these modeling experiments was to question the mobility of chloride isotopes in snow, based on the advection-diffusion approach proposed by Delmas et al. (2004). Their modeling experiment implicitly considers all ^{36}Cl to be in a mobile phase. Yet this does not allow to maintain the double-peak structure and the deep and sub-surface concentrations, nor is it entirely compatible with the fine structures observed in our data. This suggests once again that a non-mobile phase of chloride is present in snow.

4.3 Mobile vs immobile anthropogenic ^{36}Cl at Vostok

4.3.1 $^{36}\text{Cl}/\text{Cl}$ as an indicator of stratospheric anthropogenic ^{36}Cl inputs

Despite being affected by major remobilization, the ^{36}Cl concentration record at Vostok exhibits high frequency variabilities similar to those of the Cl^- and Na^+ concentrations over the entire sequence. This is particularly apparent after 1980 when the ^{36}Cl concentration starts to decrease, with an average 3.3 year variability for the more recent part of the record (Figures 5A and 5B). Such similarities are also evidenced when comparing Na^+ concentration to ^{10}Be concentration along the same snow pit (Baroni et al., 2011) (Figures 5C and 5D), and have likewise been identified with ^3H (Fourré et al., 2018). It has been proposed that these periodicities within the 3-7 year band result from a modulation of atmospheric circulation in the troposphere, induced either by the Antarctic Circumpolar

Wave (ACW) (Baroni et al., 2011) or by the Southern Annular Mode (SAM) (Fourré et al., 2018). In this scenario, the coupling between $^{10}\text{Be}/^3\text{H}$ and Na^+ is seen as an indirect link related to the influence of modes of atmospheric circulation (ACW or SAM) on stratospheric inputs (Baroni et al., 2011; Fourré et al., 2018). It has recently been shown that only a minor contribution of ^{10}Be coming from the stratosphere, on the order of 2%, is sufficient to explain the ^{10}Be snow signal at Dome C (Baroni et al., 2019). Since the $^{10}\text{Be}/^{36}\text{Cl}$ production ratio is close to 10 at all altitudes or latitudes, and since the maximum of production is in the polar stratosphere (Poluianov et al., 2016), we can reasonably assume that the main source of naturally-produced ^{36}Cl deposited at Vostok is the stratosphere. This would also apply to anthropogenic ^{36}Cl because it has been transported through the stratosphere from the low latitudes to the pole in a way similar to that of ^{137}Cs , ^{90}Sr , ^{240}Pu and ^3H , also produced during the period of nuclear bomb tests. On the other hand, chlorine (Cl^-) originates from the ocean and is transported into the troposphere, while the stratospheric source of Cl^- can be disregarded. In addition, the natural contribution of ^{36}Cl coming from the ocean is negligible whereas the $^{36}\text{Cl}/\text{Cl}^-$ ratio is estimated at 5×10^{-16} in the global ocean (Argento et al., 2010), which is more than 3 orders of magnitude lower than the 1.30×10^{-12} pre-bomb $^{36}\text{Cl}/\text{Cl}^-$ estimated at Talos Dome.

To overcome this common variability between the concentrations of ^{36}Cl and Cl^- , we normalized the ^{36}Cl data using the Cl^- concentrations determined by isotopic dilution. This normalization is based on the use of the $^{36}\text{Cl}/\text{Cl}^-$ ratio in order to isolate the anthropogenic ^{36}Cl originating in the stratosphere from the tropospheric ^{36}Cl . Normalization was applied in both the Talos Dome and Vostok snow pits, and the results are presented in Figures 6A and 6B, respectively.

There is a good correspondence between the $^{36}\text{Cl}/\text{Cl}^-$ ratio and the inventory of nuclear bomb tests (Table 1) at both Talos Dome and Vostok, taking into account a 3-year delay between the emission of ^{36}Cl at the time of the nuclear tests and the measurements of ^{36}Cl concentration in snow (Figure 6). This 3 year shift is in agreement with the estimated 3 to 4 year residence time of anthropogenic ^{36}Cl in the stratosphere (Heikkila et al., 2009b). Details of the nuclear bomb tests are presented in Table 1, with only explosions with a yield above 0.1 MT being considered. At Talos Dome, two main peaks are identified in 1955 and 1961 (Figure 6A) which can be linked to the two most powerful nuclear projects of Castel and Hardtack, at Bikini and Enewetak Atolls (11°N) (see Table 1). The values then decrease, reaching the lowest values in 1980, despite being interrupted twice by anthropogenic ^{36}Cl contributions: firstly, between 1965 and 1967 due to the Dominic project at Christmas and Johnston Islands (17°N) and then between 1970 and 1974 due to the French tests in Mururoa and Fangataufa Atolls (22°S) (Figure 6A).

The high resolution of Vostok data allows to identify accurately the major tests of Bikini/Enewetak and Christmas and Johnston Islands (Figure 6B), with major increases of the $^{36}\text{Cl}/\text{Cl}^-$ ratio corresponding to the marine nuclear test periods. The less powerful tests conducted at Mururoa and Fangataufa (22°S) are more difficult to detect due to their lower yields, and they cannot be distinguished from other peaks observed further afield which are not linked to any tests. The $^{36}\text{Cl}/\text{Cl}^-$ ratio decreases from 1968 to 2007 albeit at a slower rate than at Talos Dome and, as discussed previously, evidences post-depositional remobilization of a part of the anthropogenic ^{36}Cl in the firn. The uncertainty related to the Vostok chronology as well as the estimated 3 year shift must be kept in mind when interpreting the $^{36}\text{Cl}/\text{Cl}^-$ ratio. For example, for the major $^{36}\text{Cl}/\text{Cl}^-$ increase in 1958 which is assumed to be related to the 1956 Redwing project tests (Table 1), the delay is only approximately 2 years.

Along the Vostok record, high ^{36}Cl concentration synchronous with a transitory increase in Cl^- and Na^+ concentrations is observed in 1957 (Figure 7). Although coincidental with the 1956 solar particle event (SPE) (Gold & Palmer, 1956), this ^{36}Cl concentration increase is not reflected in the $^{36}\text{Cl}/\text{Cl}^-$ ratio record (Figure 7). This most likely reveals a period favorable to the deposition of both natural sea salt, as shown in a peak of Na^+ concentration up to 78 ppb, and ^{36}Cl at Vostok. An increase of the $^{36}\text{Cl}/\text{Cl}^-$ ratio is, however, observed in 1957.5 (Figure 7). Nevertheless, when the 3 year shift corresponding to the estimated residence time of anthropogenic ^{36}Cl in the stratosphere is applied, this ratio becomes synchronous with the 1954 Castel project nuclear tests at Bikini and Enewetak Atolls (Table 1).

4.3.2 Immobile anthropogenic ^{36}Cl

The detection of the $^{36}\text{Cl}/\text{Cl}^-$ peaks confirms that part of the deposition of anthropogenic ^{36}Cl is not mobile in snow. Indeed, the H^{36}Cl remobilization previously presented would completely remove or smooth the various ^{36}Cl pulses deposited in the 1950s and 1960s, and would therefore not be detected at Vostok. The fact that the detected $^{36}\text{Cl}/\text{Cl}^-$ ratio peaks are synchronous with the nuclear test inventory shows that when the 3 year atmospheric transport is integrated, this fraction may be immobile upon its deposition in snow, with no major time lag registered. Three possibilities may explain this immobile phase:

i) Part of the nuclear signal deposited is in particulate form, i.e. as Na^{36}Cl , contrary to findings by Zerle et al. (1997), and this portion is not totally transformed into H^{36}Cl during transport or in the snowpack. The Na^{36}Cl aerosol may be preserved in the stratosphere during its transport to Antarctica, and then only partially fractionated in the troposphere before being deposited in the snow. This would result in both anthropogenic Na^{36}Cl and H^{36}Cl in the Vostok snowpack. This Na^{36}Cl is probably transferred to Antarctica from the

stratosphere rather than from the ocean, due to the lengthy ocean circulation which would prevent ^{36}Cl from reaching Antarctica within 3 years, and also because of the estimated low ^{36}Cl oceanic reservoir that would dilute the anthropogenic ^{36}Cl (Argento et al., 2010).

ii) Part of the gaseous H^{36}Cl is not mobile after being deposited and preserved. The presence of dust may explain this preservation. Indeed, Röthlisberger et al. (2003) have shown that the presence of dust at a concentration above 20 ppb in the atmosphere prevents NaCl from fractionating by neutralizing HNO_3 and H_2SO_4 acids, thus maintaining a Cl^-/Na^+ ratio close to the emission value of 1.9 in Dome C snow. This is particularly visible during the last glacial maximum due to the fivefold concentration of dust compared with interglacial levels. The presence of dust deposited in the snowpack may also allow to neutralize part of the deposited H^{36}Cl , which is an acid like HNO_3 and H_2SO_4 , and prevent its mobility in snow layers. However, measurements made in this Vostok snow pit show a low dust concentration level for the last 60 years (at approximately 10 ppb), and no direct link between the variability of ^{36}Cl and that of the dust with a very low regression coefficient ($r^2 = 0.03$) (Jean Robert Petit, personal communication), nor with Cl^- concentration ($r^2 = 0.07$), which prevents us from concluding that the immobile phase is related to the presence of dust.

iii) Na^{36}Cl injected into the stratosphere is partially photolyzed to perchlorate (ClO_4^-) and then deposited at Vostok. Perchlorate is chemically stable (Parker, 2009) and has been measured in the ice core records of WAIS Divide in Antarctica (Crawford et al., 2017). It is naturally produced in the atmosphere (troposphere and stratosphere) due to the photolysis of chlorine species (Dasgupta et al., 2006; Sturchio et al., 2009; Jackson et al., 2010; Peterson et al., 2015a, 2015b; Crawford et al., 2017). Sturchio et al. (2009) proposed that

Accepted Article

during marine nuclear tests, anthropogenic Na^{36}Cl injected into the stratosphere may have induced a $^{36}\text{ClO}_4^-$ bomb pulse that could be detected in various environments. Considering that perchlorate is immobile in the snowpack after deposition, part of the immobile $^{36}\text{ClO}_4^-$ anthropogenic signal could be identified at Vostok. Nevertheless, perchlorate concentration measurements made at WAIS Divide show that the concentration level is at least 1000 times lower than the chloride concentration (Crawford et al., 2017). This suggests that the $^{36}\text{ClO}_4^-$ fraction may be negligible compared to the $\text{Na}^{36}\text{Cl}/\text{H}^{36}\text{Cl}$ anthropogenic fractions, and therefore not detectable at Vostok.

The nuclear imprint at Vostok thus includes both a mobile and an immobile signature. Because of the post depositional issues at Vostok and the presence of two different signatures, it is difficult to make a perfect correspondence between the individual tests and the $^{36}\text{Cl}/\text{Cl}^-$ ratio values. However, such a correspondence is expected to be feasible at other sites lacking post depositional mobility, for example at Talos Dome, provided that a sufficient sampling resolution is available.

This ratio enables for the first time to accurately identify the most powerful nuclear bomb tests in an ice core/snow record, which is not possible using the ^{36}Cl concentration only. Because anthropogenic ^{36}Cl is transported into the stratosphere, it is thought that the $^{36}\text{Cl}/\text{Cl}^-$ ratio allows to discriminate between the stratospheric and tropospheric ^{36}Cl reservoirs. The ^{36}Cl reservoir is located in the polar stratosphere, which opens perspectives for the interpretation of the ^{36}Cl produced naturally in the atmosphere.

5. CONCLUSION

In this study, ^{36}Cl concentration evolution as a function of depth in snow pits at Talos Dome and Vostok has been established over the nuclear bomb testing period. This provides information on ^{36}Cl signal behavior through the first meters of the snowpack. At Talos Dome, similar to what has been observed at Berkner Island and Dye 3, the input signal is well preserved. However, at Vostok the recorded ^{36}Cl signal evidences remobilization of a part of gaseous H^{36}Cl in the first meters of the firn due to its mobility in sites experiencing low accumulation rates, as is also observed regarding natural chloride concentration. HCl mobility is a major phenomenon affecting the first meters of the Vostok snow, while another chlorine fraction is immobile and preserved in the snow. However, the mobile fraction leads to a re-emission from the snowpack, meaning that the Vostok atmosphere is still contaminated by ^{36}Cl produced during the nuclear bomb tests from the 1950s to the 1970s.

We also show that it is necessary to compare ^{36}Cl concentrations to Cl^- concentrations determined by isotopic dilution. This is because in natural conditions, when ^{36}Cl and Cl^- concentrations are significantly correlated, the observed ^{36}Cl variations may be related to tropospheric modulations and not necessarily to ^{36}Cl production changes in the atmosphere. Knowing the Cl^- concentration allows to use the $^{36}\text{Cl}/\text{Cl}^-$ ratio to differentiate stratospheric sources from tropospheric sources during the nuclear period, and enables for the first time to detect each major nuclear event.

Finally, this study shows that ^{36}Cl concentration records at sites experiencing low snow accumulation rates must be handled with care. Indeed, gaseous H^{36}Cl is progressively lost by re-emission from the snowpack, which impacts the ^{36}Cl record along the first meters of the firn. However, below a critical depth which can be determined using the Cl^-/Na^+ ratio, only

the immobile ^{36}Cl remains. ^{36}Cl concentration can therefore be interpreted to evidence natural variation of ^{36}Cl production. More investigation is required at other sites with low snow accumulation rates that date from outside the period of nuclear bomb testing in order to permit comparison with sites with higher accumulation rates which prevent the loss of gaseous H^{36}Cl .

ACKNOWLEDGMENTS

The data are available in the supporting material. This study is a contribution to the VOLSOL (ANR-09-BLAN-0003-01) and the VANISH (ANR-07-VULN-013) projects which are funded by the Agence Nationale de la Recherche (ANR). This work has also been supported by the European Research Council under the European Union's Seventh Framework Program (FP7/2007-2013)/ERC grant agreement no. 306045. The fieldwork at Vostok benefited from logistical support from the Russian Antarctic Expeditions (RAE) with the valuable contribution of J.-R. Petit and V. Lipenkov. The Talos Dome Ice core Project (TALDICE), a joint European program, is funded by national contributions from Italy, France, Germany, Switzerland and the United Kingdom. Primary logistical support was provided by PNRA at Talos Dome. This is TALDICE publication n°56. We thank the TALDICE logistic and drilling team. We thank P. Ginot and V. Lucaire for the ion chromatography facility at IGE. The ASTER AMS national facility (CEREGE, Aix-en-Provence) is supported by the INSU/CNRS, the ANR through the "Programme d'Investissements d'Avenir" (EQUIPEX project "ASTER-CEREGE") and by the IRD.

6. REFERENCES

- Argento, D. C., Stone, J. O., Keith Fifield, L., & Tims, S. G. (2010). Chlorine-36 in seawater. *Nuclear Instruments and Methods in Physics Research Section B: Beam Interactions with Materials and Atoms*, 268(7-8), 1226-1228. <https://doi.org/10.1016/j.nimb.2009.10.139>
- Arnold, M., Aumaître, G., Bourlès, D. L., Keddadouche, K., Braucher, R., Finkel, R. C., ... Merchel, S. (2013). The French accelerator mass spectrometry facility ASTER after 4years: Status and recent developments on ³⁶Cl and ¹²⁹I. *Nuclear Instruments and Methods in Physics Research Section B: Beam Interactions with Materials and Atoms*, 294, 24-28. <https://doi.org/10.1016/j.nimb.2012.01.049>
- Bard, E., Raisbeck, G. M., Yiou, F., & Jouzel, J. (1997). Solar modulation of cosmogenic nuclide production over the last millennium: comparison between ¹⁴C and ¹⁰Be records. *Earth and Planetary Science Letters*, 150(3-4), 453-462.
- Baroni, M., Bard, E., Petit, J.-R., Magand, O., & Bourlès, D. (2011). Volcanic and solar activity, and atmospheric circulation influences on cosmogenic ¹⁰Be fallout at Vostok and Concordia (Antarctica) over the last 60years. *Geochimica et Cosmochimica Acta*, 75(22), 7132-7145. <https://doi.org/10.1016/j.gca.2011.09.002>
- Baroni, M., Bard, E., Petit, J.-R., Viseur, S., & Team, A. (2019). Persistent draining of the stratospheric ¹⁰Be reservoir after the Samalas volcanic eruption (1257 AD). *Journal of Geophysical Research: Atmospheres*.
- Baumgartner, S., Beer, J., Masarik, J., Wagner, G., Meynadier, L., & Synal, H.-A. (1998). Geomagnetic modulation of the ³⁶Cl flux in the GRIP ice core, Greenland. *Science*, 279(5355), 1330-1332.
- Bazin, L., Landais, A., Lemieux-Dudon, B., Toyé Mahamadou Kele, H., Veres, D., Parrenin, F., ... Wolff, E. (2013). An optimized multi-proxy, multi-site Antarctic ice and gas orbital chronology (AICC2012): 120-800 ka. *Climate of the Past*, 9(4), 1715-1731. <https://doi.org/10.5194/cp-9-1715-2013>

Beer, J., Johnsen, S. J., Bonani, G., Finkel, R. C., Langway, C. C., Oeschger, H., ... Woelfli, W. (1992).

¹⁰Be as time markers in polar ice cores. *The Last Deglaciation: Absolute and Radiocarbon Chronologies. NATO ASI Series*, 1(2), 141–153.

Beer, J., Siegenthaler, U., Bonani, G., Finkel, R. C., Oeschger, H., Suter, M., & Wölfli, W. (1988).

Information on past solar activity and geomagnetism from ¹⁰Be in the Camp Century ice core. *Nature*, 331(6158), 675.

Benassai, S., Becagli, S., Gragnani, R., Magand, O., Proposito, M., Fattori, I., ... Udisti, R. (2005). Sea-

spray deposition in Antarctic coastal and plateau areas from ITASE traverses. *Annals of Glaciology*, 41, 32–40.

Bentley, H. W., Phillips, F. M., & Davis, S. N. (1986). Chlorine-36 in the terrestrial environment.

Handbook of environmental isotope geochemistry, 2, 427–480.

Bentley, H. W., Phillips, F. M., Davis, S. N., Gifford, S., Elmore, D., Tubbs, L. E., & Gove, H. E. (1982).

Thermonuclear ³⁶Cl pulse in natural water. *Nature*, 300(5894), 737.

Berggren, A.-M., Beer, J., Possnert, G., Aldahan, A., Kubik, P., Christl, M., ... Vinther, B. M. (2009). A

600-year annual ¹⁰Be record from the NGRIP ice core, Greenland. *Geophysical Research Letters*, 36(11).

Bouchez, C., Pupier, J., Benedetti, L., Deschamps, P., Guillou, V., Keddadouche, K., ... Bourlès, D.

(2015). Isotope Dilution-AMS technique for ³⁶Cl and Cl determination in low chlorine content waters. *Chemical Geology*, 404, 62–70.

<https://doi.org/10.1016/j.chemgeo.2015.03.022>

Braucher, R., Keddadouche, K., Aumaître, G., Bourlès, D. L., Arnold, M., Pivot, S., ... Bard, E. (2018).

Chlorine measurements at the 5MV French AMS national facility ASTER: Associated external uncertainties and comparability with the 6MV DREAMS facility. *Nuclear Instruments and*

Methods in Physics Research Section B: Beam Interactions with Materials and Atoms, 420, 40

-45. <https://doi.org/10.1016/j.nimb.2018.01.025>

Caiazzo, L., Becagli, S., Frosini, D., Giardi, F., Severi, M., Traversi, R., & Udisti, R. (2016). Spatial and temporal variability of snow chemical composition and accumulation rate at Talos Dome site (East Antarctica). *Science of The Total Environment*, 550, 418-430.

<https://doi.org/10.1016/j.scitotenv.2016.01.087>

Christl, M., Vockenhuber, C., Kubik, P. W., Wacker, L., Lachner, J., Alfimov, V., & Synal, H.-A. (2013). The ETH Zurich AMS facilities: Performance parameters and reference materials. *Nuclear Instruments and Methods in Physics Research Section B: Beam Interactions with Materials and Atoms*, 294, 29-38. <https://doi.org/10.1016/j.nimb.2012.03.004>

Crawford, T. Z., Kub, A. D., Peterson, K. M., Cox, T. S., & Cole-Dai, J. (2017). Reduced perchlorate in West Antarctica snow during stratospheric ozone hole. *Antarctic Science*, 29(3), 292–296.

Dasgupta, P. K., Dyke, J. V., Kirk, A. B., & Jackson, W. A. (2006). Perchlorate in the United States. Analysis of relative source contributions to the food chain. *Environmental science & technology*, 40(21), 6608–6614.

De Angelis, M., & Legrand, M. (1995). Preliminary investigations of post depositional effects on HCl, HNO₃, and organic acids in polar firn layers. In *Ice core studies of global biogeochemical cycles* (p. 361–381). Springer.

Delmas, R. J., Beer, J., Synal, H. A., Muscheler, R., Petit, J.-R., & Pourchet, M. (2004). Bomb-test ³⁶Cl measurements in Vostok snow (Antarctica) and the use of ³⁶Cl as a dating tool for deep ice cores. *Tellus B*, 56(5), 492–498.

Ekaykin, A. A., Lipenkov, V. Y., Kuzmina, I. N., Petit, J. R., Masson-Delmotte, V., & Johnsen, S. J. (2004). The changes in isotope composition and accumulation of snow at Vostok station, East Antarctica, over the past 200 years. *Annals of Glaciology*, 39, 569–575.

Elmore, D., Tubbs, L. E., Newman, D., Ma, X. Z., Finkel, R., Nishiizumi, K., ... Andree, M. (1982). ³⁶Cl bomb pulse measured in a shallow ice core from Dye 3, Greenland. *Nature*, 300(5894), 735.

Feely, H. W., Seitz, H., Lagomarsino, R. J., & Biscaye, P. E. (1966). Transport and fallout of stratospheric radioactive debris. *Tellus*, 18(2-3), 316–328.

Finkel, R. C., Nishiizumi, K., Elmore, D., Ferraro, R. D., & Gove, H. E. (1980). ^{36}Cl in polar ice, rainwater and seawater. *Geophysical research letters*, 7(11), 983–986.

Fouillé, E., Landais, A., Cauquoin, A., Jean-Baptiste, P., Lipenkov, V., & Petit, J.-R. (2018). Tritium records to trace stratospheric moisture inputs in Antarctica. *Journal of Geophysical Research: Atmospheres*.

Ginot, P., Dumont, M., Lim, S., Patris, N., Taupin, J.-D., Wagnon, P., ... Laj, P. (2014). A 10 year record of black carbon and dust from a Mera Peak ice core (Nepal): variability and potential impact on melting of Himalayan glaciers. *The Cryosphere*, 8(4), 1479-1496.
<https://doi.org/10.5194/tc-8-1479-2014>

Gold, T., & Palmer, D. R. (1956). The solar outburst, 23 February 1956. Observations by the Royal Greenwich Observatory. *Journal of Atmospheric and Terrestrial Physics*, 8(4-5), 287–291.

Green, J. R., Cecil, L. D., Synal, H.-A., Kreutz, K. J., Wake, C. P., Naftz, D. L., & Frape, S. K. (2000). Chlorine-36 and cesium-137 in ice-core from mid-latitude glacial sites in the Northern Hemisphere. *Nuclear Instruments and Methods in Physics Research B*, 172, 812-816.

Hall, J. S., & Wolff, E. W. (1998). Causes of seasonal and daily variations in aerosol sea-salt concentrations at a coastal Antarctic station. *Atmospheric Environment*, 32(21), 3669–3677.

Hara, K., Nakazawa, F., Fujita, S., Fukui, K., Enomoto, H., & Sugiyama, S. (2014). Horizontal distributions of aerosol constituents and their mixing states in Antarctica during the JASE traverse. *Atmospheric Chemistry and Physics*, 14(18), 10211-10230.
<https://doi.org/10.5194/acp-14-10211-2014>

Hara, K., Osada, K., Kido, M., Hayashi, M., Matsunaga, K., Iwasaka, Y., ... Fukatsu, T. (2004). Chemistry of sea-salt particles and inorganic halogen species in Antarctic regions: Compositional differences between coastal and inland stations. *Journal of Geophysical Research: Atmospheres*, 109(D20).

Heikkilä, U., Beer, J., & Feichter, J. (2009a). Meridional transport and deposition of atmospheric ^{10}Be . *Atmospheric Chemistry and Physics*, 9(2), 515–527.

Heikkilä, U., Beer, J., Feichter, J., Alifimov, V., Synal, H.-A., Schotterer, U., ... Thompson, L. (2009b).

³⁶Cl bomb peak: comparison of modeled and measured data. *Atmospheric chemistry and physics*, 9(12), 4145–4156.

Iizuka, Y., Ohno, H., Uemura, R., Suzuki, T., Oyabu, I., Hoshina, Y., ... Motoyama, H. (2016). Spatial distributions of soluble salts in surface snow of East Antarctica. *Tellus B: Chemical and Physical Meteorology*, 68(1), 29285. <https://doi.org/10.3402/tellusb.v68.29285>

Iizuka, Y., Tsuchimoto, A., Hoshina, Y., Sakurai, T., Hansson, M., Karlin, T., ... Fujita, S. (2012). The rates of sea salt sulfatization in the atmosphere and surface snow of inland Antarctica: SEA SALT SULFATIZATION IN ANTARCTICA. *Journal of Geophysical Research: Atmospheres*, 117(D4), n/a-n/a. <https://doi.org/10.1029/2011JD016378>

Jackson, W. A., Böhlke, J. K., Gu, B., Hatzinger, P. B., & Sturchio, N. C. (2010). Isotopic composition and origin of indigenous natural perchlorate and co-occurring nitrate in the southwestern United States. *Environmental science & technology*, 44(13), 4869–4876.

Jourdain, B., & Legrand, M. (2002). Year-round records of bulk and size-segregated aerosol composition and HCl and HNO₃ levels in the Dumont d'Urville (coastal Antarctica) atmosphere: Implications for sea-salt aerosol fractionation in the winter and summer. *Journal of Geophysical Research*, 107(D22). <https://doi.org/10.1029/2002JD002471>

Koide, M., Goldberg, E. D., Herron, M. M., & Langway Jr, C. C. (1977). Transuranic depositional history in South Greenland firn layers. *Nature*, 269(5624), 137.

Koide, M., Michel, R., Goldberg, E. D., Herron, M. M., & Langway Jr, C. C. (1979). Depositional history of artificial radionuclides in the Ross Ice Shelf, Antarctica. *Earth and Planetary Science Letters*, 44(2), 205–223.

Legrand, M., & Delmas, R. J. (1988). Formation of HCl in the Antarctic atmosphere. *Journal of Geophysical Research: Atmospheres*, 93(D6), 7153–7168.

Legrand, M., Preunkert, S., Wolff, E., Weller, R., Jourdain, B., & Wagenbach, D. (2017). Year-round records of bulk and size-segregated aerosol composition in central Antarctica (Concordia

site)—Part 1: Fractionation of sea-salt particles. *Atmospheric Chemistry and Physics*, 17(22), 14039.

Masarik, J., & Beer, J. (1999). Simulation of particle fluxes and cosmogenic nuclide production in the Earth's atmosphere. *Journal of Geophysical Research: Atmospheres*, 104(D10), 12099–12111.

Mayewski, P. A., & Legrand, M. (1990). Recent increase in nitrate concentration of Antarctic snow. *Nature*, 346(6281), 258.

Miyake, F., Horiuchi, K., Motizuki, Y., Nakai, Y., Takahashi, K., Masuda, K., ... Matsuzaki, H. (2019). ^{10}Be Signature of the Cosmic Ray Event in the 10th Century CE in Both Hemispheres, as Confirmed by Quasi-Annual ^{10}Be Data From the Antarctic Dome Fuji Ice Core. *Geophysical Research Letters*, 46(1), 11–18.

Mulvaney, R., Oerter, H., Peel, D. A., Graf, W., Arrowsmith, C., Pasteur, E. C., ... Miners, W. D. (2002). 1000 year ice-core records from Berkner Island, Antarctica. *Annals of Glaciology*, 35, 45–51.

Nishiizumi, K., Arnold, J. R., Elmore, D., Ma, X., Newman, D., & Gove, H. E. (1983). ^{36}Cl and ^{53}Mn in Antarctic meteorites and ^{10}Be - ^{36}Cl dating of Antarctic ice. *Earth and Planetary Science Letters*, 62(3), 407–417.

Osman, M., Das, S. B., Marchal, O., & Evans, M. J. (2017). Methanesulfonic acid (MSA) migration in polar ice: data synthesis and theory. *The Cryosphere*, 11(6), 2439–2462.

<https://doi.org/10.5194/tc-11-2439-2017>

Oyabu, I., Iizuka, Y., Wolff, E., & Hansson, M. (2016). Chemical composition of soluble and insoluble particles around the last termination preserved in the Dome C ice core, inland Antarctica. *Climate of the Past Discussions*, 1–22. <https://doi.org/10.5194/cp-2016-42>

Parker, D. R. (2009). Perchlorate in the environment: the emerging emphasis on natural occurrence. *Environmental Chemistry*, 6(1), 10–27.

Pedro, J. B., McConnell, J. R., van Ommen, T. D., Fink, D., Curran, M. A., Smith, A. M., ... Das, S. B.

(2012). Solar and climate influences on ice core ^{10}Be records from Antarctica and Greenland during the neutron monitor era. *Earth and Planetary Science Letters*, 355, 174–186.

Peterson, K., Cole-Dai, J., Brandis, D., Cox, T., & Splett, S. (2015a). Rapid measurement of perchlorate in polar ice cores down to sub-ng L⁻¹ levels without pre-concentration. *Analytical and bioanalytical chemistry*, 407(26), 7965–7972.

Peterson, K., Cole-Dai, J., Brandis, D. L., & Manandhar, E. (2015b). Assessment of anthropogenic contribution to perchlorate in the environment using an ice core record. *Emerging Micro-Pollutants in the Environment: Occurrence, Fate, and Distribution*, 175–185.

Poluianov, S. V., Kovaltsov, G. A., Mishev, A. L., & Usoskin, I. G. (2016). Production of cosmogenic isotopes ^7Be , ^{10}Be , ^{14}C , ^{22}Na , and ^{36}Cl in the atmosphere: Altitudinal profiles of yield functions: COSMOGENIC ISOTOPES IN THE ATMOSPHERE. *Journal of Geophysical Research: Atmospheres*, 121(13), 8125–8136. <https://doi.org/10.1002/2016JD025034>

Pourchet, M., Bartarya, S. K., Maignan, M., Jouzel, J., Pinglot, J. F., Aristarain, A. J., ... Preiss, N. (1997). Distribution and fall-out of ^{137}Cs and other radionuclides over Antarctica. *Journal of Glaciology*, 43(145), 435–445.

Pourchet, M., Magand, O., Frezzotti, M., Ekaykin, A., & Winther, J.-G. (2003). Radionuclides deposition over Antarctica. *Journal of Environmental Radioactivity*, 68, 137–158.

Raisbeck, G. M., Cauquoin, A., Jouzel, J., Landais, A., Petit, J.-R., Lipenkov, V. Y., ... Yiou, F. (2017). An improved north–south synchronization of ice core records around the 41 kyr ^{10}Be peak. *Climate of the Past*, 13(3), 217–229. <https://doi.org/10.5194/cp-13-217-2017>

Raisbeck, G. M., Yiou, F., Fruneau, M., Loiseaux, J. M., Lieuvin, M., & Ravel, J. C. (1981). Cosmogenic $^{10}\text{Be}/^7\text{Be}$ as a probe of atmospheric transport processes. *Geophysical Research Letters*, 8(9), 1015–1018.

Raisbeck, G. M., Yiou, F., Jouzel, J., & Petit, J. R. (1990). ^{10}Be and $\delta^2\text{H}$ in polar ice cores as a probe of the solar variability's influence on climate. *Phil. Trans. R. Soc. Lond. A*, 330(1615), 463–470.

- Raisbeck, G. M., Yiou, F., Jouzel, J., Petit, J. R., Barkov, N. I., & Bard, E. (1992). ^{10}Be deposition at Vostok, Antarctica during the last 50,000 years and its relationship to possible cosmogenic production variations during this period. *NATO ASI Series, I 2*, 127-139.
- Rankin, A. M., Auld, V., & Wolff, E. W. (2000). Frost flowers as a source of fractionated sea salt aerosol in the polar regions. *Geophysical Research Letters*, *27*(21), 3469–3472.
- Rankin, A. M., Wolff, E. W., & Mulvaney, R. (2004). A reinterpretation of sea-salt records in Greenland and Antarctic ice cores? *Annals of Glaciology*, *39*, 276–282.
- Röthlisberger, R., Mulvaney, R., Wolff, E. W., Hutterli, M. A., Bigler, M., De Angelis, M., ... Udisti, R. (2003). Limited dechlorination of sea-salt aerosols during the last glacial period: Evidence from the European Project for Ice Coring in Antarctica (EPICA) Dome C ice core. *Journal of Geophysical Research: Atmospheres*, *108*(D16).
- Sasa, K., Matsushi, Y., Tosaki, Y., Tamari, M., Takahashi, T., Nagashima, Y., ... Motoyama, H. (2010). Measurement of cosmogenic ^{36}Cl in the Dome Fuji ice core, Antarctica: Preliminary results for the Last Glacial Maximum and early Holocene. *Nuclear Instruments and Methods in Physics Research Section B: Beam Interactions with Materials and Atoms*, *268*(7-8), 1193-1196. <https://doi.org/10.1016/j.nimb.2009.10.131>
- Sigl, M., Fudge, T. J., Winstrup, M., Cole-Dai, J., Ferris, D., McConnell, J. R., ... Sowers, T. A. (2016). The WAIS Divide deep ice core WD2014 chronology – Part 2: Annual-layer counting (0–31 ka BP). *Climate of the Past*, *12*(3), 769-786. <https://doi.org/10.5194/cp-12-769-2016>
- Stenni, B., Buiron, D., Frezzotti, M., Albani, S., Barbante, C., Bard, E., ... Udisti, R. (2011). Expression of the bipolar see-saw in Antarctic climate records during the last deglaciation. *Nature Geosciences*, *4*, 46-49.
- Sturchio, N. C., Caffee, M., Beloso Jr, A. D., Heraty, L. J., Böhlke, J. K., Hatzinger, P. B., ... Dale, M. (2009). Chlorine-36 as a tracer of perchlorate origin. *Environmental science & technology*, *43*(18), 6934–6938.

- Synal, H.-A., Beer, J., Bonani, G., Suter, M., & Wölfli, W. (1990). Atmospheric transport of bomb-produced ^{36}Cl . *Nuclear Instruments and Methods in Physics Research Section B: Beam Interactions with Materials and Atoms*, 52(3-4), 483–488.
- Thompson, L. G., Mosley-Thompson, E., Davis, M. E., Henderson, K. A., Brecher, H. H., Zagorodnov, V. S., ... Hardy, D. R. (2002). Kilimanjaro ice core records: evidence of Holocene climate change in tropical Africa. *science*, 298(5593), 589–593.
- Veres, D., Bazin, L., Landais, A., Toyé Mahamadou Kele, H., Lemieux-Dudon, B., Parrenin, F., ... Wolff, E. W. (2013). The Antarctic ice core chronology (AICC2012): an optimized multi-parameter and multi-site dating approach for the last 120 thousand years. *Climate of the Past*, 9(4), 1733-1748. <https://doi.org/10.5194/cp-9-1733-2013>
- Wagenbach, D., Ducroz, F., Mulvaney, R., Keck, L., Minikin, A., Legrand, M., ... Wolff, E. (1998). Sea salt aerosol in coastal Antarctic regions. *Journal of Geophysical Research*, 103, 10,961-10,974. <https://doi.org/doi:10.1029/97JD01804>
- Wagon, P., Delmas, R. J., & Legrand, M. (1999). Loss of volatile acid species from upper firn layers at Vostok, Antarctica. *Journal of Geophysical Research: Atmospheres*, 104(D3), 3423–3431.
- Whitlow, S., Mayewski, P. A., & Dibb, J. E. (1992). A comparison of major chemical species seasonal concentration and accumulation at the South Pole and Summit, Greenland. *Atmospheric Environment. Part A. General Topics*, 26(11), 2045–2054.
- Winkler, R., Landais, A., Risi, C., Baroni, M., Ekaykin, A., Jouzel, J., ... Falourd, S. (2013). Interannual variation of water isotopologues at Vostok indicates a contribution from stratospheric water vapor. *Proceedings of the National Academy of Sciences*, 110(44), 17674–17679.
- Yiou, F., Raisbeck, G. M., Baumgartner, S., Beer, J., Hammer, C., Johnsen, S., ... Stievenard, M. (1997). Beryllium 10 in the Greenland ice core project ice core at summit, Greenland. *Journal of Geophysical Research: Oceans*, 102(C12), 26783–26794.

Zerle, L., Faestermann, T., Knie, K., Korschinek, G., Nolte, E., Beer, J., & Schotterer, U. (1997). The ^{41}Ca bomb pulse and atmospheric transport of radionuclides. *Journal of Geophysical Research: Atmospheres*, 102(D16), 19517–19527.

Accepted Article

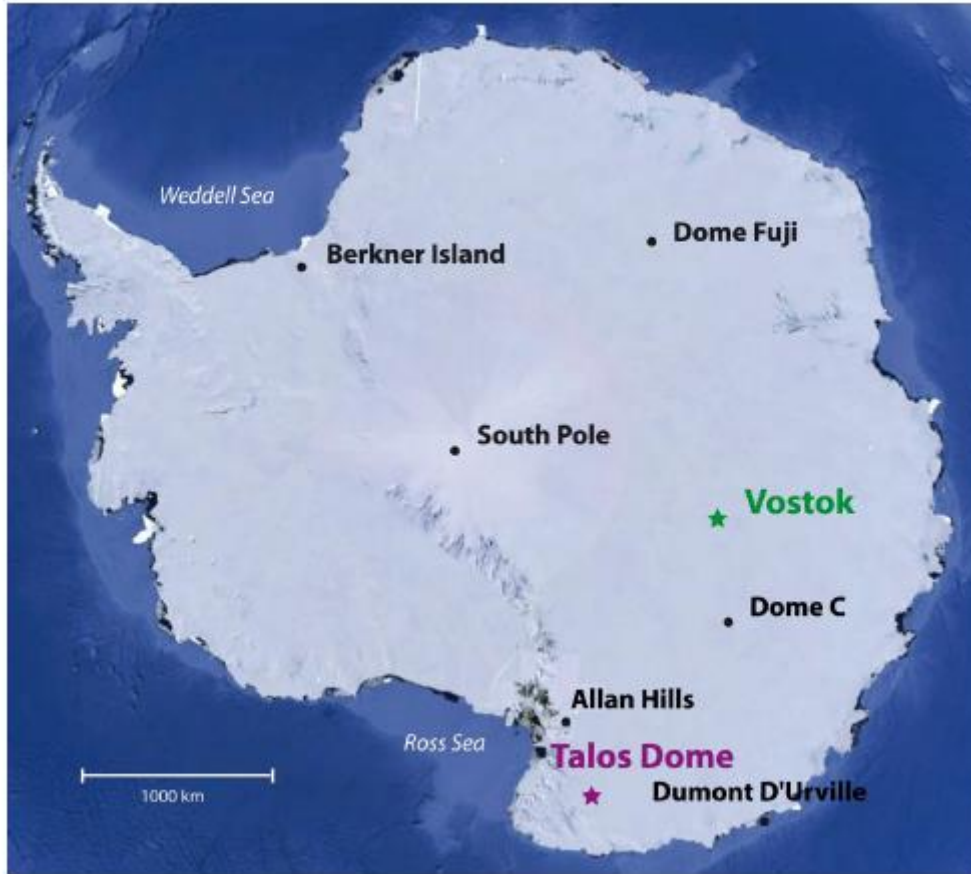


Figure 1. Map of Antarctica representing the different sites listed in this manuscript (dots). Vostok and Talos Dome (stars), represent the sites at which ^{36}Cl measurements were performed (modified from Google Earth).

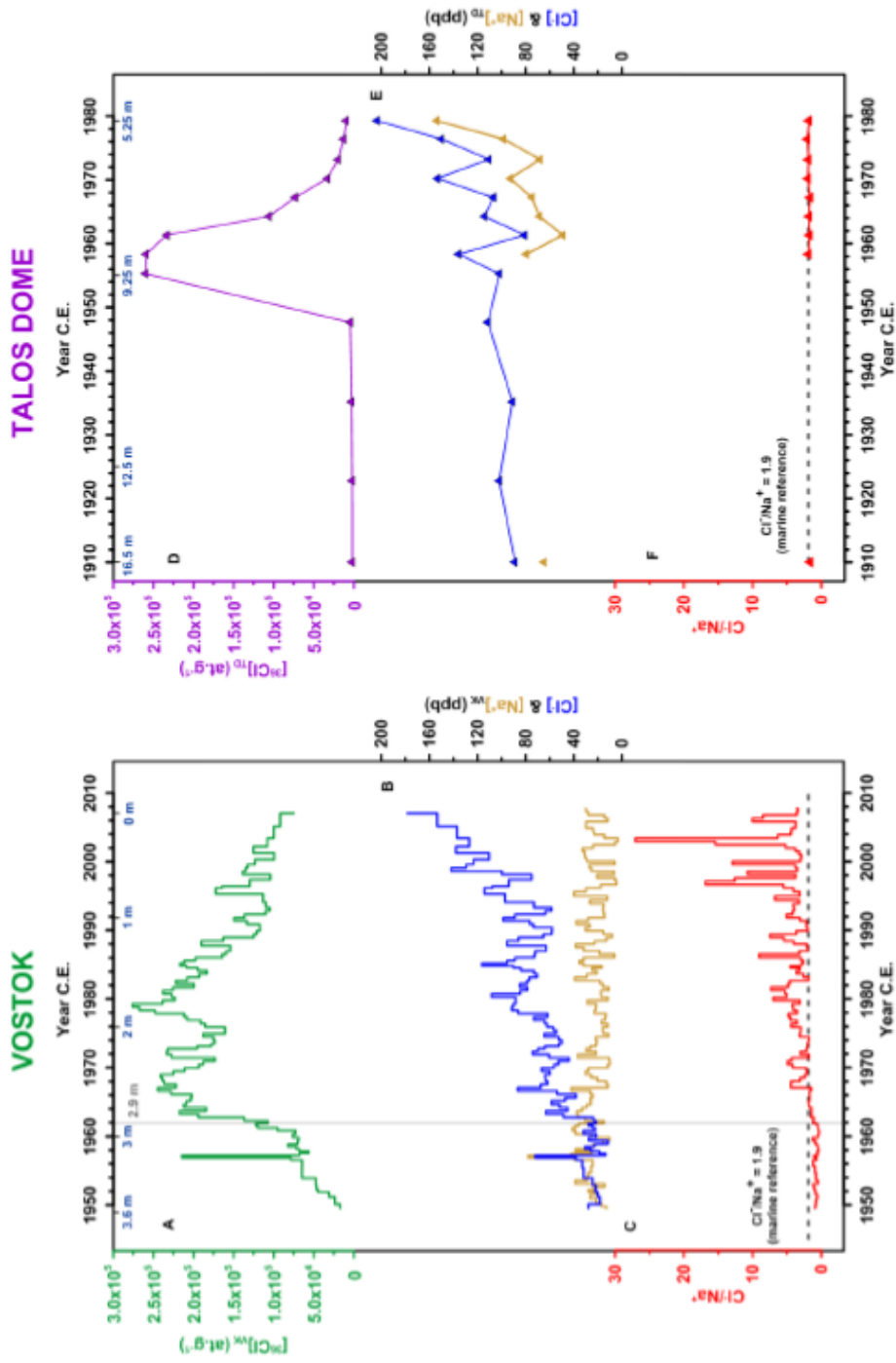


Figure 2. The ^{36}Cl record, Cl^- and Na^+ concentration and the Cl^-/Na^+ ratio for Vostok (left panel) and Talos Dome (right panel) reported as a function of time. Na^+ concentration data for Vostok have previously been published (Baroni et al., 2011). The Cl^-/Na^+ ratio is compared with the marine reference of 1.9 estimated by Legrand et al. (2017), and is

represented by the dotted line. Note that the time scale is different between the two panels, with the Vostok record covering the 1950 to 2010 period, while the Talos Dome record covers the 1910 to 1980 period. The chloride concentration presented here results from the isotopic dilution method, but the Cl^-/Na^+ ratio has been estimated using chromatography measurements. For Talos Dome, four samples were not measured using chromatography, as can be observed in the gap between 1910 and 1958 for Na^+ concentration and the Cl^-/Na^+ ratio. The grey line for the Vostok panel represents the limit at which Cl^-/Na^+ ratio values seem constant, at depths greater than 2.9 m.

Accepted Article

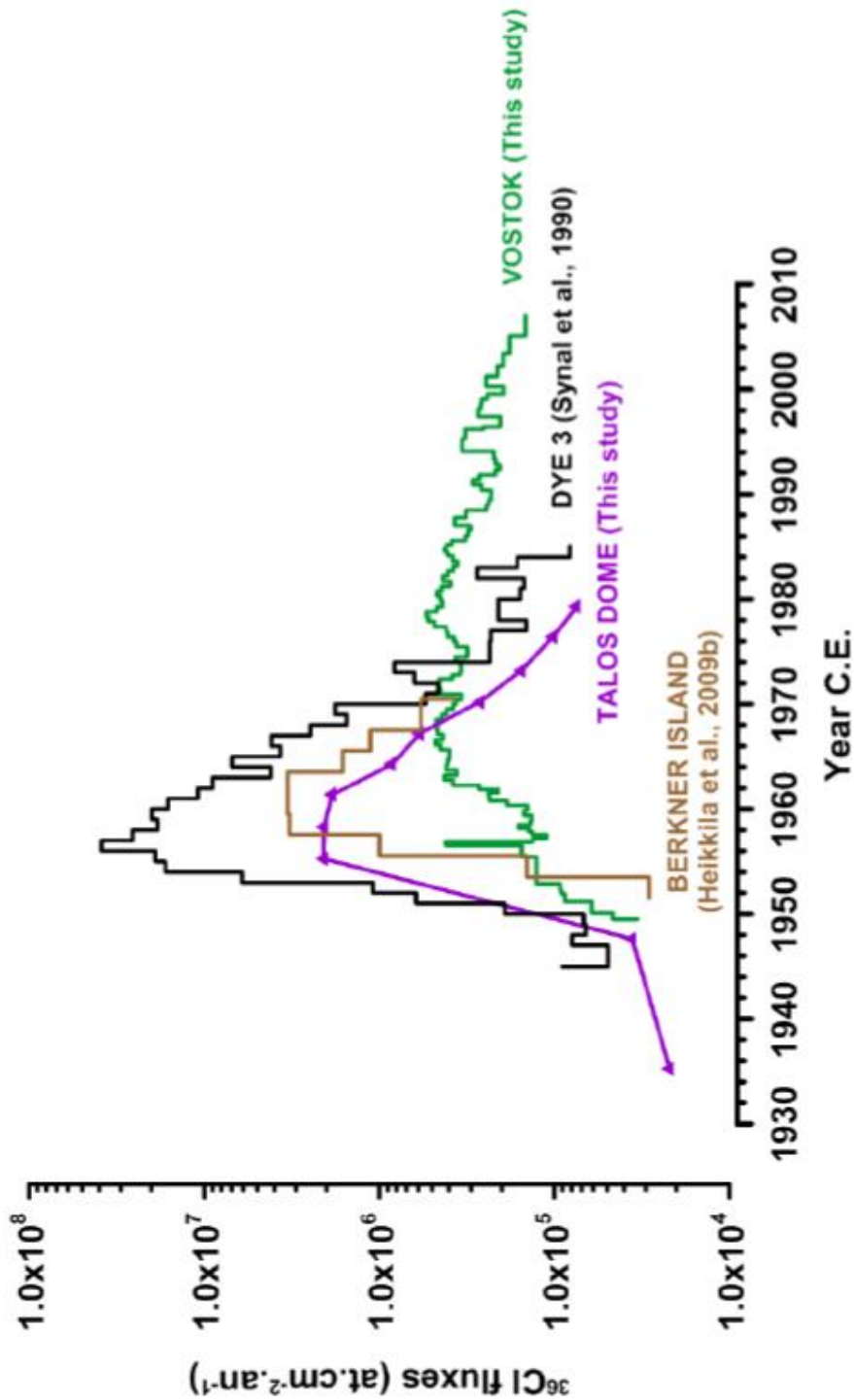


Figure 3. ^{36}Cl fluxes measured at Vostok and Talos Dome during the nuclear bomb testing period compared with ^{36}Cl fluxes at Dye 3 in Greenland (Synal et al., 1990) and at Berkner Island in Antarctica (Heikkila et al., 2009b). The ^{36}Cl data of Dye 3 and Berkner Island have been corrected using the new value of the standard used at ETH Zurich, where the samples were measured (Christl et al., 2013).

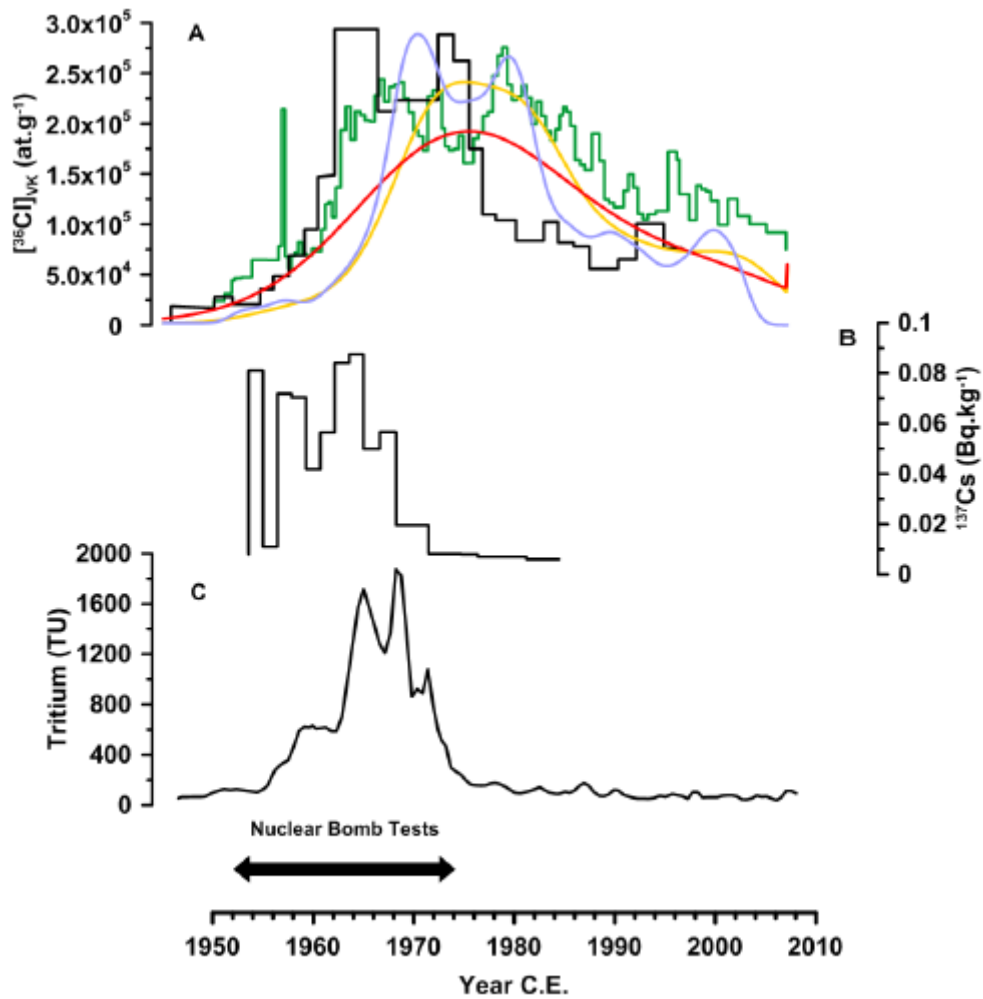


Figure 4. ^{36}Cl evolution through time from this study (green line) compared to ^{36}Cl concentration of Vostok in another snow pit dug and measured 10 years prior to our study (Delmas et al., 2004, in black), but also in comparison with ^{137}Cs (B) (Baroni et al., 2011) and ^3H (C) (Fourré et al., 2018) from the same snow pit. The ^{36}Cl model simulation is also represented, with the orange line reflecting the values of advection and diffusion proposed by Delmas et al. 2004, the red line illustrating new parameters fitting better with our ^{36}Cl values, and the purple line representing a reduced diffusion coefficient compared to the other two simulations.

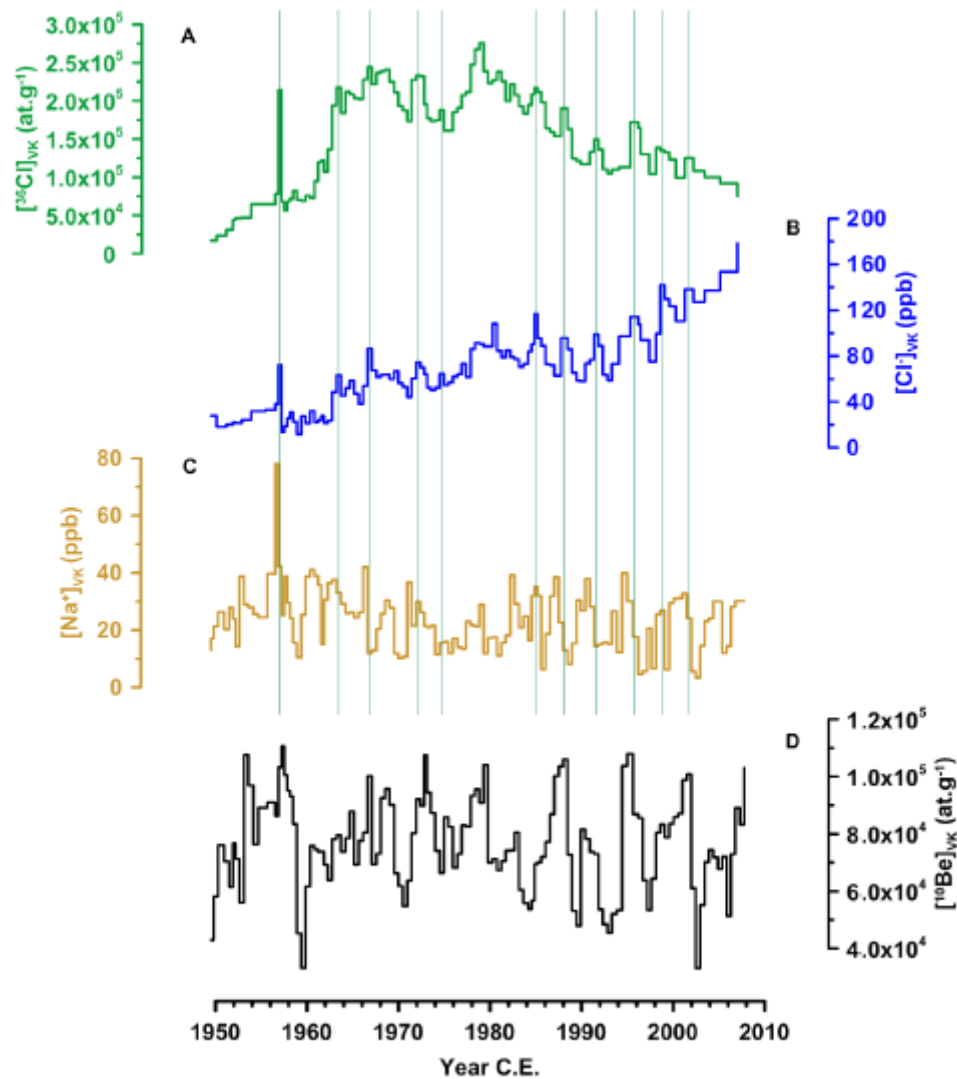


Figure 5. Representation of the correspondence of ^{36}Cl and Cl^- concentrations marked with the green vertical lines (A and B), as well as with the sodium concentration (C). The ^{10}Be data are also reported (D) and were corrected from the two main volcanic eruptions of the last 60 years: the Agung eruption in 1963 and the Pinatubo event in 1991 (Baroni et al., 2011).

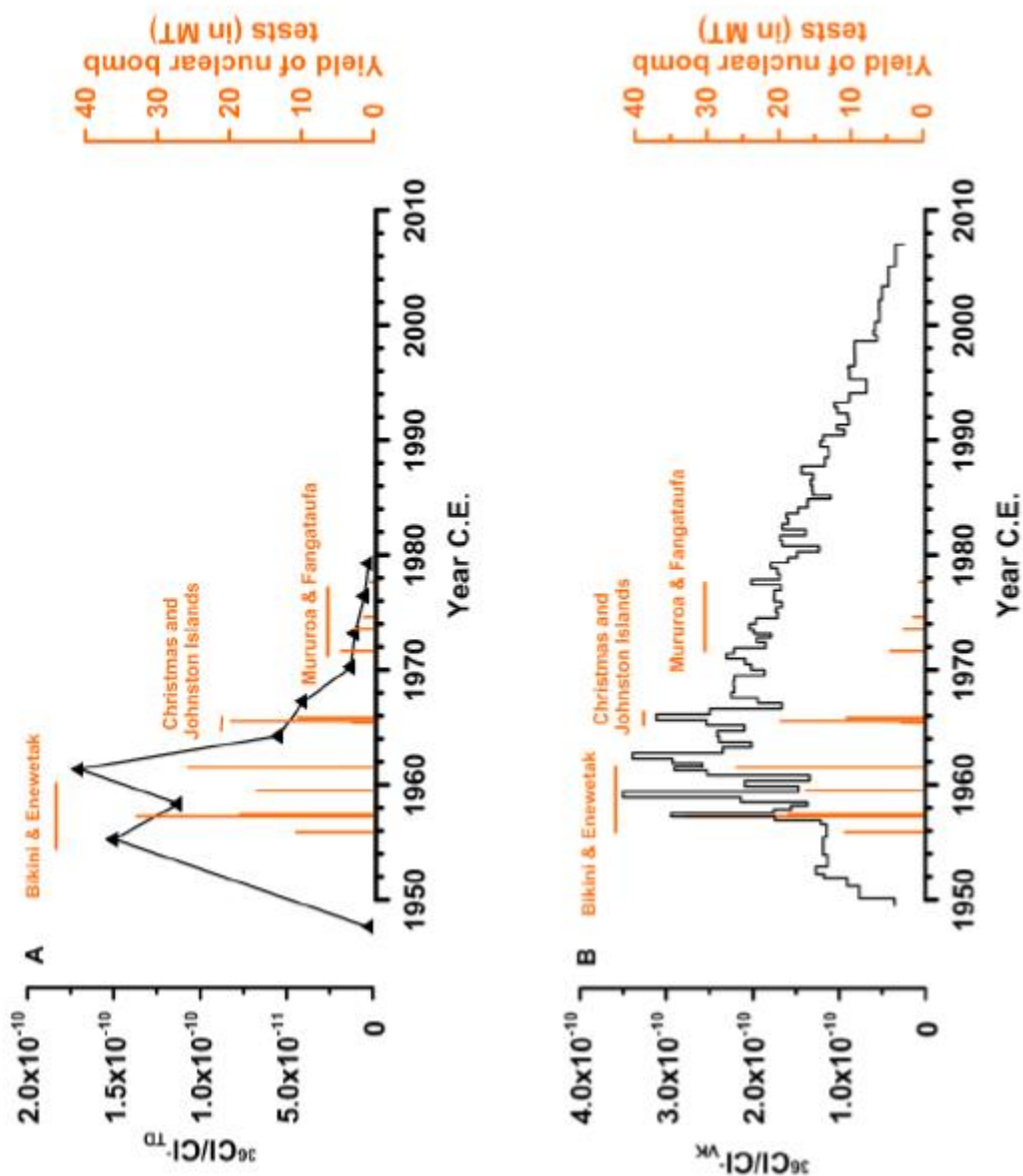


Figure 6. $^{36}\text{Cl}/\text{Cl}$ ratio for Talos Dome (A) and Vostok (B) records in comparison with nuclear marine bomb tests expressed in MT (See Table 1). We calculated the sum of the yields when different tests occurred in the same year. All the tests referenced have yields above 100 kt. The emission dates were shifted by 3 years from the emission time referenced in Table 1, to take into account the estimated 3 year residence time of ^{36}Cl in the stratosphere prior to deposition in the Antarctic snow (Heikkila et al., 2009b). Only 10 of the 13 Talos Dome data points are reported in the upper panel, which focusses on the 1950 - 2010 period to enable better visualization of the nuclear bomb period.

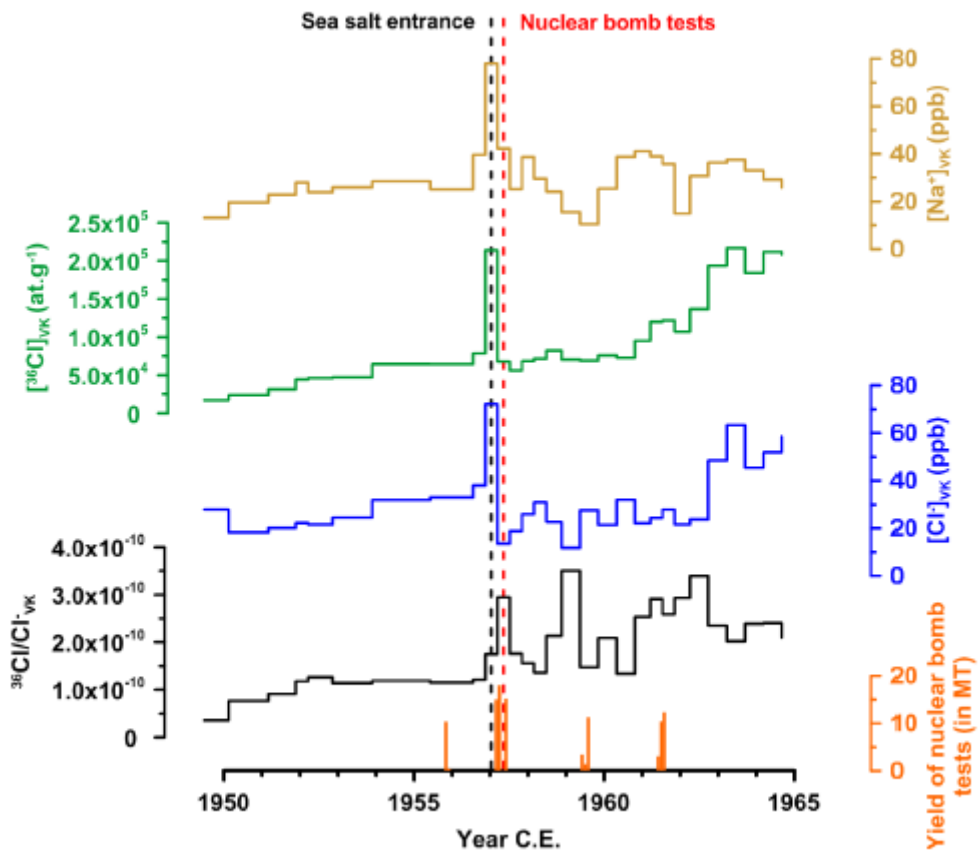


Figure 7. Representation of the 1950 to 1965 period exploring the simultaneous increase in Na^+ , ^{36}Cl and Cl^- concentration in 1957, as observed at Vostok. The $^{36}\text{Cl}/\text{Cl}^-$ ratio is also reported with marine nuclear bomb tests in MT (see Table 1). The tests were shifted by 3 years and a monthly mean was applied from the nuclear bomb test list referenced in Table 1.

Table 1. Nuclear bomb tests leading to a ^{36}Cl stratospheric contribution with corresponding location. All the tests referenced have yields above 100 kt, with bold values above 3 MT (https://inis.iaea.org/collection/NCLCollectionStore/_Public/31/060/31060372.pdf).

<i>Year</i>	<i>Month</i>	<i>Location</i>	<i>Project</i>	<i>Test</i>	<i>Explosive yield (MT)</i>
1952	10	Enewetak	Ivy	Mike	10.4
	11	Enewetak		King	0.5
1954	2	Bikini	Castel	Bravo	15
	3	Bikini		Romeo	11
	4	Bikini		Koon	0.11
	4	Bikini		Union	6.9
	5	Bikini		Yankee	13.5
	5	Enewetak		Nectar	1.69
	5	Bikini		Zuni	3.5
1956	6	Bikini	Redwing	Flathead	0.365
	6	Bikini		Dakota	1.1
	7	Enewetak		Apache	1.85
	7	Bikini		Navajo	4.5
	7	Bikini		Tewa	5
1958	5	Bikini	Hardtack	Fir	1.36
	5	Enewetak		Koa	1.37
	5	Enewetak		Yellow wood	0.33
	6	Bikini		Maple	0.213
	6	Bikini		Aspen	0.0319
	6	Enewetak		Walnut	0.0145
	6	Bikini		Redwood	0.412
	6	Enewetak		Elder	0.88
	6	Enewetak		Oak	8.9
	7	Bikini		Cedar	0.22
	7	Enewetak		Dogwood	0.397
	7	Bikini		Poplar	9.3
	7	Enewetak		Pisonia	0.255
	7	Enewetak		Olive	0.202
7	Enewetak	Pine	2		
1962	4	Christmas Island	Dominic	Adobe	0.19
	4	Christmas Island		Aztec	0.41
	5	Christmas Island		Arkansas	1.1
	5	Christmas Island		Questa	0.67
	5	Christmas Island		Yukon	0.1

	5	Christmas Island		Encino	0.5
	6	Christmas Island		Alma	0.782
	6	Christmas Island		Truckee	0.21
	6	Christmas Island		Yeso	3
	6	Christmas Island		Harlem	1.2
	6	Christmas Island		Rinconada	0.8
	6	Christmas Island		Bighorn	7.7
	6	Christmas Island		Bluestone	1.3
	7	Christmas Island		Sunset	1
	7	Christmas Island		Pamlico	3.9
	10	Johnston Island		Chama	1.6
	10	Johnston Island		Calamity	0.8
	10	Johnston Island		Housatonic	8.3
1968	7	Mururoa		Capella	0.115
	7	Mururoa		Castor	0.45
	8	Mururoa		Pollux	0.15
	8	Fangataufa		Canopus	2.6
	9	Mururoa		Procyon	1.3
1970	5	Mururoa		Cassiopée	0.224
	5	Fangataufa		Dragon	0.945
	7	Mururoa		Licorne	0.914
	8	Mururoa		Toucan	0.594
1971	6	Mururoa		Encelade	0.44
	8	Mururoa		Rh�a	0.955
1974	7	Mururoa		G�meaux	0.15
	8	Mururoa		Scorpion	0.096
	9	Mururoa		Verseau	0.332

Location	Coordinates
Enewetak	11.35°N, 162.35°E
Bikini	11.30°N, 162.30°E
Christmas Island (Kiribati)	2.00°N, 157.25°W
Johnston Island	17.18°N, 169.45°W
Mururoa	21.50°S, 138.55°W
Fangataufa	22.15°S, 138.45°W